J Comp Physiol A (1996) 178: 579–604

ORIGINAL PAPER

M. Schmidt · B. W. Ache

Processing of antennular input in the brain of the spiny lobster, *Panulirus argus*

I. Non-olfactory chemosensory and mechanosensory pathway of the lateral and median antennular neuropils

Accepted: 28 August 1995

Abstract Neurons in the brain of the spiny lobster that respond to chemical and mechanical stimulation of the antennule (antenna I) were recorded and stained intracellularly. Described here are neurons that do not arborize in the olfactory and accessory lobes of the deutocerebrum, but rather primarily target the lateral and/or the median antennular neuropils of the deutocerebrum. Some of the neurons also extend into the antennal and tegumentary neuropils of the tritocerebrum and the neuropils of the median protocerebrum. Included are antennular sensory afferents, antennular motoneurons, projection neurons descending from the central brain, projection neurons ascending from the central brain and projection neurons descending from the eyestalk ganglia. Collectively, these neurons consitutute a novel antennular sensory pathway that is parallel to and independent of the antennular olfactory pathway. The novel pathway integrates mechanosensory and non-olfactory chemosensory information in the lateral and/or the median antennular neuropils, which also serve as lower motor centers of the antennule. Division of the arthropod deutocerebrum into two, functionally distinct chemosensory pathways may reflect differences in how chemosensory information is processed that is fundamental to understanding the origin of the sense of smell.

Key words Crustacean · Chemoreception · Mechanoreception · Deutocerebrum · Motoneurons · Projection neurons

M. Schmidt (✉)
Institut für Biologie, TU Berlin, Franklinstrasse 28/29, D-10587 Berlin, Germany

M. Schmidt · B. W. Ache
Whitney Laboratory, University of Florida, St. Augustine, FL 32086, USA

B. W. Ache
Departments of Zoology and Neuroscience, University of Florida, St. Augustine, FL 32086, USA

Abbreviations *AC* anterior cluster (cluster 6, 7) · *AL* accessory lobe · *aMC* anterior subcluster of medial cluster (cluster 9) · *AnN* antenna II (antennal) neuropil · A_INv main antenna I (antennular) nerve · A_INM antenna I (antennular) motor nerve · $A_{II}Nv$ main antenna II (antennal) nerve · $A_{II}NM$ antenna II (antennal) motor nerve · *DCN* deutocerbral commissure neuropil · *dDLC* dorsal subcluster of dorsal lateral cluster (cluster 15) · *dDUMC* dorsal subcluster of dorsal unpaired median cluster (cluster 17) · *DUGC* dorsal unpaired globuli cell cluster · *LAN* lateral antenna I (antennular) neuropil · *IDUMC* lateral subcluster of dorsal unpaired median cluster (cluster 16) · *LF* lateral flagellum of antenna I (antennule) · *MAN* median antenna I (antennular) neuropil · *mDUMC* median subcluster of dorsal unpaired median cluster (cluster 17) · *MF* medial flagellum of antenna I (antennule) · *MPN* anterior and posterior median protocerebral neuropils · *OC* oesophageal connective · *OCM* oculomotor nerve · *OL* olfactory lobe · *PT* protocerebral tract · *TN* tegumentary neuropil · *TNv* tegumentary nerve · *vDLC* ventral subcluster of dorsal lateral cluster (cluster 14) · *VPALC* ventral paired anterolateral cluster (cluster 8) · *VUMC* ventral unpaired median cluster (cluster 13) · *AMP* adenosine monophosphate · *ASC* L-ascorbic acid · *ASW* artificial sea water · *BET* betaine HCl · *M1* mixture 1 (TAU, BET, ASC, NH4) · *M2* mixture 2 (SUC, NIC, AMP, TMA) · *M3* mixture 3 (M1, M2, PRO) · NH_4 NH_4Cl · *NIC* nicotinic acid · *PRO* L-proline · *SUC* sucrose · *TAU* taurine · *TM* TetraMarin extract · *TMA* trimethylamine HCl

Introduction

The brain of decapod crustaceans, like that of other anthropods, is divided into three major regions, each receiving direct sensory input from one of the three major head appendages. The deutocerebrum receives input from the biramous antennule (antenna I), the appendage bearing the olfactory organ (Sandeman and Denburg 1976; Mellon and Munger 1990; Schmidt and Ache 1992; Schmidt et al. 1992). There are four major deutocerebral neuropils – the paired olfactory lobes (OL), the paired accessory lobes (AL – missing or reduced in some families), the paired lateral antennular (antenna I) neuropils (LAN), and the unpaired median antennular (antenna I) neuropil (MAN) (Helm 1928; Blaustein et al. 1988; Sandeman et al. 1992). The OL and AL are glomerular neuropils and contrast with the LAN, which is stratified, and the MAN, which is unstructured (Sandeman and Luff 1973; Blaustein et al. 1988; Schmidt et al. 1992). The majority of deutocerebral input comes from aesthetasc sensilla – delicate, hair-like sensilla with a porous cuticle that exclusively occur on the lateral flagellum of the antennule and comprise the olfactory organ (e.g. Grünert and Ache 1988). However, other types of sensilla on the medial and lateral flagella are also chemosensory (Fuzessery 1978; Tierney et al. 1988). These non-olfactory sensilla are smooth, conical hairs of different sizes which have a terminal pore and innervation suggestive of dual, chemo-/mechanoreceptive function, like contact chemoreceptors in insects (Laverack 1964; Snow 1974; Gleeson 1982; Spencer and Linberg 1986; Grünert, personal communication). Other antennular sensilla are purely mechanosensory and include the chordotonal organs spanning the joints between all segments (Wyse and Maynard 1965), feathered hairs on the first basal segment (Kouyama and Shimozawa 1982; Roye and Dillaman 1982; Roye 1986), and the well-studied statocyst hairs (e.g. Sandeman and Okajima 1972; Silvey et al. 1976; Patton and Grove 1992).

How information other than statocyst input is processed in the deutocerebrum of decapods is not well understood. All the major deutocerebral neuropils with the exception of the AL receive primary sensory input (Sandeman and Okajima 1973; Sandeman and Denburg 1976; Yoshino et al. 1983; Roye 1986; Mellon and Munger 1990; Schmidt and Ache 1992; Schmidt et al. 1992). Earlier, we provided anatomical evidence suggesting that in the spiny lobster the OL is almost exclusively innervated by afferents from the aesthetascs, while the LAN is innervated by chemo- and mechanosensory afferents from dually-innervated sensilla on the flagella and the basal segments, and the input to the MAN is dominated by large mechanosensory afferents from the basal segments of the antennule and some presumptive non-olfactory chemosensory afferents (Schmidt and Ache 1992; Schmidt et al. 1992). We also provided anatomical evidence showing that motoneurons of antennular muscles arborize extensively in the LAN and MAN suggesting that these neuropils are lower motor centers (Schmidt and Ache 1993). These neuroanatomical data are consistent with an idea first put forth by Maynard (1965) that the deutocerebrum in decapod crustaceans is subdivided into two functionally-distinct sensory pathways, a primarily chemosensory (olfactory) pathway that is mediated through the OL and the AL and a primarily mechanosensory and motor pathway that is mediated through the LAN and the MAN. Yet these data suggest that Maynard's scheme may be overly simplified in that the LAN appears to receive significant chemosensory input from the antennule.

Here, we attempt to verify the functional subdivision of the deutocerebrum suggested by anatomical evidence by physiological characterizing morphologically-identified neurons that innervate the LAN/MAN and comparing their responses to neurons that innervate the OL/AL (see accompanying paper). We show that mechanosensory and non-olfactory chemosensory information are integrated in the LAN and/or MAN and that these neuropils also serve as lower motor centers of the antennule. This pathway is parallel to and independent of the antennular olfactory pathway (see accompanying paper). Part of these data have been presented earlier in abstract form (Schmidt et al. 1991).

Materials and methods

Animals

Male and female intermolt specimens of the Caribbean spiny lobster, *Panulirus argus*, with carapace lengths between 40 and 70 mm were collected in the Florida Keys and held in tanks supplied with running seawater on a diet of squid.

Preparation, recording and staining

Neurons were penetrated with microelectrodes in an excised head preparation, in which the medial artery (1 ml/min) supplying the brain and the two lateral arteries (3–4 ml/min each) supplying the antennules were continuously perfused with chilled (ca. 15°C), oxygenated spiny lobster saline (Hamilton and Ache 1983) (Fig. 1a). To minimize movements of muscles, the protocerebral tracts connecting the central brain with the eyestalk ganglia and all the brain nerves except the main antennular nerves were cut except for experiments requiring visual input, in which case the protocerebral tracts were left intact. This procedure disrupted all motoneurons except those with axons in the ventral aspect of the main antennular nerves (Schmidt and Ache 1993). In some instances, these too were eliminated after rotation of the head preparation to gain access. A micromanipulated glass platform stabilized the brain. The dorsal surface of the brain except for the area around the medial artery was desheathed.

Penetrations were targeted at the dorsal deutocerebral neuropils (LAN and MAN). Electrodes were made from 1.0 mm diameter

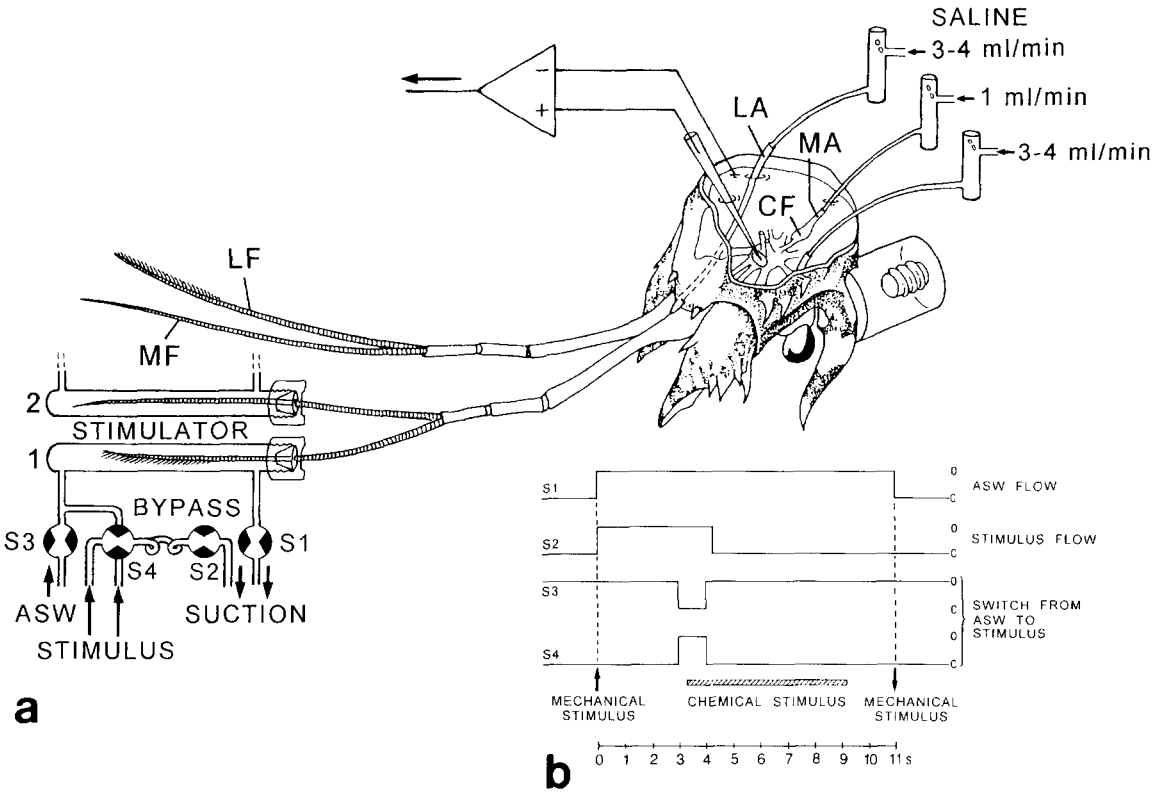

Fig. 1a Schematic drawing of the excised, perfused head preparation. Solenoid valves (*S1–S4*) shown for only one of the paired stimulators. **b** The valves are timed to draw artificial sea water (*ASW*) through the stimulator and chemical stimulus through a bypass of similar volume, which are then switched to divert the chemical stimulus over the lateral (*LF*) or medial (*MF*) flagellum of the antennule with no concomitant mechanical stimulation. *Abbreviations*: lateral artery (*LA*), medial artery (*MA*), cor frontale (*CF*)

thin-walled filament tubing (Sutter Instruments). The electrodes were filled with 0.5 *M* KCl and 0.05 *M* Tris buffer at pH 7.5 containing 4% biocytin (Sigma Chemical; Horikawa and Armstrong 1988). Electrode impedance was 30–50 MΩ, measured in the bath. The intracellular signals were amplified through a bridge circuit (Getting, Model 5) and displayed on an oscilloscope for on-line verification. The intracellular signals were digitized and stored along with appropriate timing signals and verbal commentary on a video tape recorder. The stored data were analyzed off-line using commercial data analysis software (Data Pac II, Run Technologies, Inc.) on an IBM compatible 486 computer (Gateway 2000, Inc.).

Biocytin was injected iontophoretically following recording with a continuous depolarizing 2–5 nA current for 10–60 min. An additional 10–90 min was allowed for the Biocytin to spread before the brain was fixed *in situ* by submersing it in 4% freshly prepared paraformaldehyde in 0.1 *M* Sörensen phosphate buffer (SPB) + 15% sucrose for about 30 min. The brain was then dissected out of the head preparation, postfixed in the same fixative for 16–48 h, rinsed in 0.02 *M* SPB + 3.3% NaCl (SPBS), desheathed fully, embedded in gelatin (13% in SPBS; Sigma Type A, 60 bloom), and cut on a vibratome into 100 µm thick, horizontal sections. The free floating sections were treated according to the procedure by Schmidt et al. (1992) and visualized by an avidin-biotinylated horseradish peroxidase complex (ABC; Vector Labs)/diaminobenzidine (DAB; Sigma Chemical). Stained sections were transferred to gelatinized slides, dried at room temperature over night and coverslipped with Permount (Fisher Scientific) after dehydration in an alcohol series and incubation in xylene. Some of the sections were counterstained by incubation in 0.2% OsO_4 for 15–30 min prior to dehydration.

Stained neurons were viewed, photographed and traced with brightfield optics and camera-lucida (Nikon Optiphot and Olympus BHM-2). Neurons were reconstructed from serial vibratome sections by tracing stained profiles in all sections individually at 225×, aligning the tracings visually and drawing the combined profiles as viewed from dorsal perspective, i.e., ventral profiles are broken by more dorsal ones. Attempts were made to preserve proportionality as much as possible, but the finest branches had to be drawn considerably greater than their original thickness and in neurons with many fine arborizations, the finest branches were omitted for clarity. Reconstructed neurons are shown with their major arborizations on the right side of the brain regardless of their actual position in the preparation.

Stimulation

The lateral and medial flagella of the ipsilateral antennule were stimulated chemically and mechanically by two independent stimulators (Fig. 1a). Each stimulator consisted of a teflon tube (inner diameter, 2 mm), one end of which was closed and the other of which was sealed around the antennular flagella with a conical sleeve of silicone. Artificial seawater (ASW, pH 7.8) or chemical stimuli (see below) were drawn over the distal one-half of the flagella at 10 ml/min using the following paradigm (Fig. 1b): (1) start ASW to provide mechanical stimulation (onset indicated by an upward arrow in the recordings) and concurrently start stimulus solution into a bypass loop, (2) after 3 s delay, exchange flows for 1 s so that the stimulus solution flows over the flagellum with minimum

mechanical artifact and (3) after 11 s delay, terminate the flow over the flagellum (offset indicated by a downward arrow in the recordings). Stream spreading limited the peak concentration inside the tube to ca. 30% of the introduced (reported) concentration, as determined by conductivity measurements. The stimulus exceeded half-maximal concentration from ca. 0.3 s to 5.3 s after switching to the stimulus flow. This 5 s interval was considered as the effective stimulus period and is indicated by a hatched bar in the recordings.

Chemical stimuli consisted of: L-proline (PRO), betaine HCl (BET), taurine (TAU), L-ascorbic acid (ASC), nicotinic acid (NIC), adenosine monophosphate (AMP), sucrose (SUC), trimethylamine HCl (TMA), and NH_4Cl (NH_4). The substances were presented alone or in one of three different mixtures: M1-TAU, BET, ASC, NH_4; M2-SUC, NIC, AMP, TMA; and M3 – all nine substances. Stock solutions of each substance were prepared in ASW at 1 *M*, stored frozen in aliquots, and diluted at least two orders of magnitude in ASW prior to use. An extract of the fish food TetraMarin (TM, Tetra Werke) and female lobster urine were also tested as stimuli. TM was dissolved in ASW at 2 g/60 ml, centrifugated and filtered. Aliquots were stored frozen and diluted 1:10 with ASW prior to the experiments. Urine was collected from female specimens of *P. argus* by inserting a thin polyethylene tubing into the opening of a maxillary gland and evacuating the bladder. The urine of 20 animals was pooled, stored frozen in aliquots and diluted 1:10 prior to the expeiments. Chemicals were obtained from Sigma Chemical.

Experimental protocol

Given a stable impalement, a neuron's response was determined to chemical and mechanical stimulation of the ipsilateral lateral antennular flagellum. Only neurons responding to at least one of the stimulus modalities were analyzed further. Neurons were screened for possible chemosensitivity with M1, M2, M3 or TM. Some neurons were tested by applying different chemicals or different concentrations of one chemical to the ipsilateral lateral flagellum. Different substances were presented in random order, while different concentrations were presented in ascending order. Other neurons were tested by applying the same chemical to the medial and lateral flagella of the ipsilateral antennule. At least 30 s elapsed between successive chemical stimuli.

Neuroanatomy

Biocytin was used to backfill the cut ends of the circumoesophageal connectives (OC), the protocerebral tracts (PT) and the oculomotor nerves (OCM). Either the whole nerve or axon bundles teased from it were placed in 6% biocytin in 0.05 *M* Tris-buffer (pH 7.4) for 2–8 h in a continuously perfused head preparation of medium sized animals (carapace length 45–70 mm). The brain was subsequently fixed and treated further as described above. The total number of labeled somata was calculated by summating the maximum counts of labeled cell bodies in different subclusters from all preparations (see Schmidt and Ache 1993). Terminology of brain neuropils, nerves and fiber tracts is according to Sandeman et al. (1992) with only minor changes in some of the abbreviation used. The terminology of Blaustein et al. (1988) with the modifications by Schmidt and Ache (1993) is used for the soma clusters. Also listed are the identification numbers given by Sandeman et al. (1992) for the soma clusters. "Brain" refers to the cephalic ganglion in its entirety, while "central brain" refers to the part of the cephalic ganglion located in the head cup, and "eyestalk ganglia" to the lateral protocerebrum and the visual neuropils of the cephalic ganglion located in the eyestalks.

Results

General characteristics of recorded neurons

Thirty-three neurons either arborized outside the OL/AL neuropils ($n = 26$) or were not filled but penetrated in the LAN ($n = 7$) (Tables 1, 2). Figure 2 depicts the neuropils collectively innervated by these neurons and the soma clusters in which their somata are located. As a group, the neurons arborized in the lateral and median antennular neuropils (LAN, MAN) of the deutocerebrum, the antenna II and the tegumentary neuropils (AnN, TN) of the tritocerebrum, and the anterior and posterior neuropils of the median protocerebrum (MPN) (Table 1, Fig. 2). None of the neurons had even minor branches in either of the deutocerebral olfactory neuropils (OL/AL). The filled neurons were entirely ($n = 19$) or primarily ($n = 7$) ipsilateral (Table 1). Their somata ranged from 27–90 μm in diameter and occurred in one of three clusters – the dorsal unpaired median cluster (DUMC, $n = 16$), the anterior subcluster of the medial cluster (aMC, $n = 2$), and the anterior cluster (AC, $n = 1$) (Table 1, Fig. 2b). Five distinct classes of neurons could be distinguished based on the location of the axon and the soma: antennular sensory afferents, antennular motoneurons, descending central brain neurons, ascending central brain neurons, and descending eyestalk neurons. Each of these classes is detailed below.

As might be expected from their diverse morphology, the neurons differed widely in spontaneous activity, action potential amplitude, and synaptic potentials (Table 2). Thirty-one of the neurons responded to stimulation of the lateral flagellum of the ipsilateral antennule; two sensory afferents responded exclusively to input from the base of the antennule. Of these, 10 were chemosensitive, two were mechanosensitive (one of them a mechanosensory afferent) and 19 were bimodal chemo-/mechanosensitive. Response profiles to both stimulus modalities could be either simple (only one response component), or complex (several response components). Chemosensory input from the lateral flagellum typically evoked "simple" phasic or phasic-tonic excitation, which lasted as long as the stimulus duration (Figs. 3d, 9c, 11e, 14d, 16b) or was much shorter (Figs. 3a, 10d, 12c, 13d, 15d, 16c). One neuron was inhibited by the chemical stimulation of the lateral flagellum (Fig. 8c) and in seven neurons the phasic excitation was followed by a longer lasting inhibition (plus a subsequent phasic excitation in two neurons) (Figs. 6d, 7d, 16a). Mechanosensory input from the lateral flagellum typically evoked a phasic excitatory burst at the onset and/or the stop of the carrier ASW flow (e.g. Figs. 6d, 7d, 12c, 13d, 14d, 16b); in four neurons this burst was followed by a longer lasting inhibition (Figs. 11e, 16a) and in one neuron it was preceded by a short inhibition (Fig. 10d). Most (12/21) of the

Table 1 Morphological properties of biocytin-filled neurons, ordered according to morphological type. *Column 1 (No.):* identification number *Column 2 (Type):* morphological type of filled neurons; ?, typification problematic. *Column 3 (Soma localization):* soma cluster of the central brain, in which the filled soma was localized or site of presumptive soma location in case the soma was not present in the sections; *LF*, lateral flagellum of antennule; *dDUMC (17), IDUMC (16), mDUMC (17)*, dorsal, lateral or median subcluster of dorsal unpaired median cluster; *AC*, anterior cluster; *aMC* (anterior subcluster of medial cluster of the olfactory deutocerebrum). *Column 4 (Soma ∅, [μm]):* soma diameter in μm, length × width; soma diameter not measured since soma not present in sections. *Column 5 (Axon local.):* localization of axon in one of the nerves or fiber tracts leaving the central brain; A_1Nv, main antennular nerve; A_1NM, antennular motor nerve; *OC*, oesophageal connective; *PT*, protocerebral tract; –, axon not present in sections. *Column 6 (Axon ∅, [μm]):* axon diameter in μm; –, axon diameter not measured. *Column 7 (Multip. fill):* presence of weakly filled neurons in addition to intracellularly recorded, strongly filled neuron; *N*, primary neurite; *A*, axon; *S*, soma; –, no additional neurons filled. *Column 8–12:* presence and extent of arborizations in neuropils on the ipsi- and the contralateral side of the central brain; +, sparse arborization; + +, dense arborization; + + +, very dense arborization; *blank*, no arborization. *Column 8 (LAN):* lateral antennular neuropil. *Colulmn 9 (MAN):* median antennular neuropil. *Column 10 (TN):* tegumentary neuropil. *Column 11 (AnN):* antennal neuropil. *Column 12 (MPN):* anterior and posterior median protocerebral neuropils

No.	Type	Soma localization	Soma ∅ [μm]	Axon local.	Axon ∅ [μm]	Multip. fill	LAN		MAN		TN		AnN		MPN	
							ipsi	con.	ipsi	con.	ipsi	con.	ipsi	con.	ipsi	con.
67	Afferent LAN	LF	–	A_1Nv	10	–	+ + +									
66	Afferent MAN	Ant. I Base	–	A_1Nv	50	–			+ +							
68	Afferent MAN	Ant. I Base	–	A_1Nv	15	–			+ +							
1	Motoneur. I	dDUMC (17)	36 × 27	A_1NM	45	–	+ +		+ +		+					
3	Motoneur. I	IDUMC (16)	60 × 75	A_1NM	30	–	+ + +		+ +		+ +				+	
4	Motoneur. I?	IDUMC (16)	66 × 75	A_1Nv	27	–	+		+		+					
5	Motoneur. I	dDUMC (17)	45 × 45	A_1Nv	30	–	+ + +		+ +		+					
6	Motoneur. I	dDUMC (17)	60 × 60	A_1Nv	30	–	+ + +		+ +		+					
9	Motoneur. I	IDUMC (16)	80 × 60	A_1NM	27	+1N/A	+ + +		+ +		+					
20	Motoneur. I	IDUMC (16)	40 × 45	A_1Nv	15	–	+ +		+ + +		+					
34	Motoneur. I	IDUMC (16)	–	A_1Nv	–	–	+ + +		+ +		+					
64	Motoneur. I	dDUMC (17)	80 × 72	A_1NM	12	+1S/N/A	+ +		+ +		+					
10	Motoneur. II	IDUMC (16)	80 × 75	A_1NM	24	–	+		+ + +		+ +					
58	Motoneur. III	IDUMC (16)	68 × 56	A_1Nv	32	+1N/A	+ + +		+							
25	Motoneur. III?	centr. brain?	–	A_1Nv	12	–	+ + +		+							
2	desc. brain	mDUMC (17)	60 × 60	OC	21	–	+ +	+ +	+	+	+		+ + +			
8	desc. brain	IDUMC (16)	90 × 92	OC	20	–	+ +		+ +	+	+	+				
12	desc. brain	AC (6 + 7)	56 × 56	OC	15	–			+ +	+	+ +		+ + +		+ + +	
24	desc. brain?	centr. brain?	–	–	–	–	+ +	+	+ +	+ +	+		+ + +		+	+
56	desc. brain	IDUMC (16)	36 × 40	OC	8	–			+	+	+ +		+ + +		+	+
62	desc. brain	IDUMC (16)	52 × 48	OC	8	–			+ +	+	+	+		+		
63	desc. brain	dDUMC (17)	52 × 60	OC	16	–	+ +		+		+ +		+		+	
26	asc. brain	aMC (9)	28 × 37	PT	12	–			+		+		+ + +		+ +	
59	asc. brain	aMC (9)	36 × 44	PT	16	+2S/N	+ + +		+		+		+ +		+ +	+
7	desc. eyest.	eyestalk	–	PT	5	–			+						+ + +	
19	desc. eyest.	eyestalk	–	PT	45	–			+		+ + +		+ +		+ +	

mechanosensory neurons responded equally to the onset and the stop of the carrier ASW flow (Figs. 11d, 12c, 13d, 14d, 16b), but eight of the cells were directionally sensitive (Figs. 3a, 6d, 7d, 10d). The remaining cell, a mechanosensory afferent originating in the lateral flagellum, responded tonically to the ASW flow (Fig. 4d).

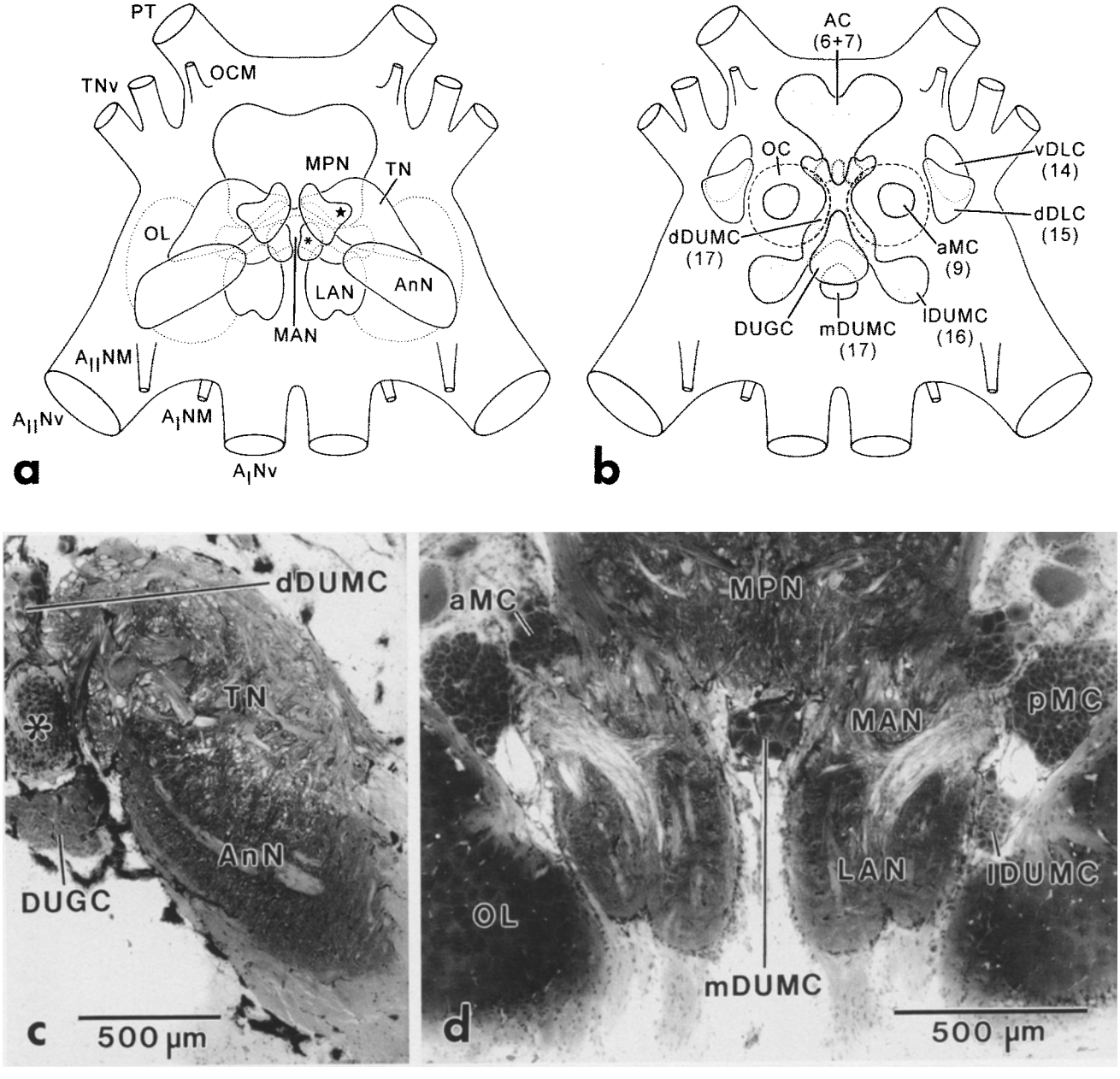

Fig. 2a–d Schematic drawings of the neuropils (**a**) and the soma clusters (**b**) in the dorsal part of the central brain of *Panulirus argus* in a horizontal orientation, dorsal view. An outline of olfactory lobe (*OL*) is provided for comparison with accompanying paper. Soma clusters containing somata of intracellularly filled neurons are lightly shaded. (**c**) LM micrograph of horizontal, ethyl gallate stained section of the tritocerebrum. Note different neuropilar structure in tegumentary neuropil (*TN*-unstructured), antennal neuropil (*AnN*-stratified) and "antennular glomeruli" (*asterisk*-glomerular). **d** LM micrograph of horizontal, ethyl gallate stained section of the deutocerebrum. Note two lobed, weakly stratified lateral antennular neuropil (*LAN*), the unstructured median antennular neuropil (*MAN*), and the unstructured neuropils of the median protocerebrum (*MPN*). *Abbreviations*: anterior cluster (*AC*), anterior subcluster of medial cluster (*aMC*), antennal neuropil (*AnN*), main antenna I (antennular) nerve (A_INv), antenna I (antennular) motor nerve (A_INM), main antenna II (antennal) nerve ($A_{II}Nv$), antenna II (antennal) motor nerve ($A_{II}NM$), dorsal subcluster of dorsal lateral cluster (*dDLC*), dorsal subcluster of dorsal unpaired median cluster (*dDUMC*), dorsal unpaired globuli cell cluster (*DUGC*), lateral antenna I (antennular) neuropil (*LAN*), lateral subcluster of dorsal unpaired median cluster (*lDUMC*), median antenna I (antennular) neuropil (*MAN*), median subcluster of dorsal unpaired median cluster (*mDUMC*), oesophageal connective (*OC*), oculomotor nerve (*OCM*), olfactory lobe (*OL*), protocerebral tract (*PT*), tegumentary neuropil (*TN*), tegumentary nerve (*TNv*), ventral subcluster of dorsal lateral cluster (*vDLC*), antennular glomeruli (*asterisk*), antennal glomeruli (*star*)

Table 2 Physiological properties of neurons, with antennular sensory input, ordered according to their morphological type. *Column 1 (No.):* identification number. *Column 2 (Fill):* +, neuron filled with biocytin; *R*, neuron reconstructed; −, neuron recorded in the LAN but not filled. *Column 3 (Type):* morphological type of filled neurons, ?, typification problematic. *Column 4 (Ampl. [mV]):* amplitude of action potentials in mV, in case of multiple spike amplitudes values for smaller action potentials are provided. *Column 5 (Spont. [Hz]):* mean spontaneous spiking activity in Hz. *Column 6 (Synaptic activity):* presence of synaptic activity in recordings; *eP*, EPSPs; *iP*, IPSPs; *MS*, multiple spike amplitudes; −, no synaptic activity visible. *Columns 7–10:* responses to sensory stimulation of the antennular flagella; *upward arrow*, excitation (increase in frequency of action potentials and/or presence of EPSPs); *downward arrow*, inhibition (decrease in frequency of action potentials and/or presence of IPSPs); *filled arrow*, strong response; *unfilled arrow*, weak response; *sequence of arrows*, complex response consisting of the indicated response components; /, delimiter between mechanosensory responses to the start (*left*) and the stop (*right*) of the ASW flow; −, no response; *blank*, stimulation not tested. *Column 7 (Mech. LF):* responses to mechanical stimulation of the lateral flagellum; *two upward arrows* (# 67), tonic response; ? (# 56), response questionable. *Column 8 (Chem. LF):* responses to chemical stimulation of the lateral flagellum. *Column 9 (Mech. MF):* responses to mechanical stimulation of the medial flagellum, *Column 10 (Chem. MF):* responses to chemical stimulation of the medial flagellum

No.	Fill	Type	Ampl. [mV]	Spont. [Hz]	Synaptic activity	Mech. LF	Chem. LF	Mech. MF	Chem. MF
67	+/R	Afferent LAN	65	0–1	–	⇑⇑	–	–	–
66	+	Afferent MAN	50	0	–	–	–		
68	+/R	Afferent MAN	55	~ 5	–	–	–		
1	+	Motoneur. I	30	10–20	–	–	⇑		
3	+/R	Motoneur. I	35	~ 5	–	⇧/⇑	⇑⇓⇧		
4	+	Motoneur. I ?	20	5–20	–	–	⇑		
5	+/R	Motoneur. I	20	20–30	–	⇑/⇧	⇧⇓⇧		
6	+	Motoneur. I	20	20–25	–	–	⇑		
9	+	Motoneur. I	30/5	5–10	eP/MS	–/⇧	⇑⇓⇧		
20	+/R	Motoneur. I	55	0	–	⇧/⇑	⇑		
34	+	Motoneur. I	80	~ 5	–	⇑/⇑	⇑⇓		
64	+/R	Motoneur. I	40	5–10	–	⇧/⇧	⇓	⇧/⇧	⇧
10	+/R	Motoneur. II	25	0	eP	–	⇑		
58	+/R	Motoneur. III	15	5–10	iP/eP	⇩⇑/–⇧	⇑	⇓⇧/⇓–	⇑
25	+	Motoneur. III?	60	~ 20	–	–	⇧⇓		
2	+	desc. brain	35/5	~ 5	MS	–	⇑		
8	+	desc. brain	35	~ 5	–	⇧/⇑	⇑		
12	+/R	desc. brain	40	5–10	–	⇑⇩/⇑⇩	⇑		
24	+/R	desc. brain?	50	0	–	⇑/⇑	⇑		
56	+/R	desc. brain	50	0	iP/MS	–	⇑	–	⇧
62	+	desc. brain	15	0	iP/eP	–⇧/–⇧	⇧	⇩⇧/–⇧	⇧
63	+	desc. brain	80	10–15	–	⇧⇩/⇧⇩	⇧	⇧⇩/⇧⇩	⇧
26	+	asc. brain	20	~ 1	–	–	⇧		
59	+/R	asc. brain	50	~ 1	eP	⇧/⇧	–	⇧/–	⇑
7	+/R	desc. eyest.	15	~ 5	iP/eP	⇧/⇧	⇑		
19	+/R	desc. eyest.	60	~ 5	–	–	⇧		
14	–		40	~ 5	–	⇧/⇧	⇧		
18	–		30	~ 5	–	⇑⇩/⇑–	⇧		
43	–		65	5–10	–	⇧⇩/⇧⇩	⇑⇓	⇧–/⇧–	⇑–
48	–		10	~ 10	eP	⇧/–	⇧⇩	–	⇑–
57	–		60	1–3	–	⇧/⇧	⇑	⇧/–	⇧
60	–		10	0	iP/eP	⇧/⇧	⇑		
69	–		20	5–10	–	–	⇑		

Chemical stimulation of the lateral flagellum elicited dose-dependent responses with thresholds of sensitivity below 1 μ*M* ($n = 4$) (Figs. 3, 14d). As a population neurons responded to all 4 mixtures (TM, M1, M2, M3), but often neurons were differentially sensitive to different mixtures (Table 3, Figs. 6d, 14d). Neurons differed in their sensitivity to single compounds from being unresponsive to all single compounds to responding to most (but not all) of the nine compounds tested (Table 3, Figs. 6d, 7d). The rank order of effectiveness of the single compounds was taurine > ascorbic acid > L-proline > AMP > betaine = TMA > nicotinic acid > ammonium chloride > sucrose. Five of seven neurons tested responded to female urine, the composition of which was unknown (Table 3, Fig. 9c).

Nine of 10 neurons that were tested for sensitivity of medial flagellum stimulation received input from the medial flagellum (one was a mechanosensory afferent of the lateral flagellum; Fig. 4) (Table 2). Two of these neurons responded only to chemical stimulation of the medial flagellum, while seven were bimodal chemo- and mechanosensitive. The responses to medial flagellum stimulation typically differed quantitatively and, in some instances, qualitatively from those evoked by lateral flagellum stimulation (Table 2, Figs. 8c, 10d, 13d, 16), the extreme being neurons that were excited

by chemical stimulation of the medial flagellum and inhibited by chemical stimulation of the lateral flagellum (Figs. 8c, 16a). The inputs typically summed when the two flagella were stimulated simultaneously (Figs. 8c, 10d, 13d, 16c), with only one hint of possible interflagellar synergism (neuron # 56, mechanosensory response).

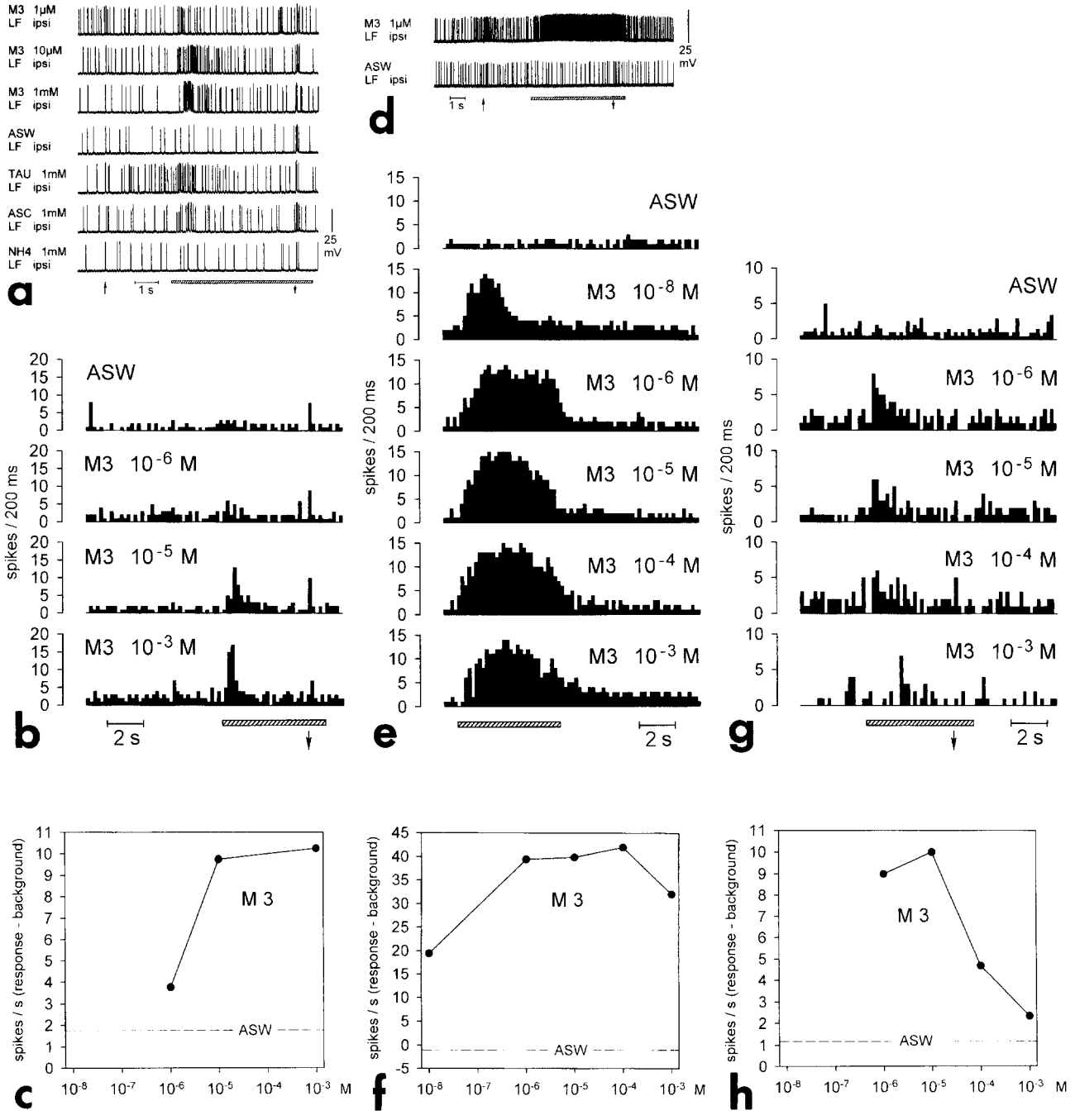

Fig. 3a–h Response of neurons in the LAN/MAN pathway to chemical stimulation of the lateral flagellum of the antennule. **a** Responses of neuron 8 to mixture 3 (*M3*, 1 μ*M* to 1 m*M*), artificial sea water (*ASW*), taurine (*TAU*), ascorbic acid (*ASC*) and Peristimulus time histograms (PSTH-bin width 200 ms) of selected responses in **a. c.** Plot of concentration-response function of the responses shown in **b**. *Abscissa*: concentration. *Ordinate*: response magnitude calculated as mean number of spikes/1s averaged over the total duration of the response to the chemical stimulus minus the number of spikes/1s before stimulation (spontaneous activity) averaged over the same period of time. **d** Responses of neuron 7 to 1 μ*M* M3 and ASW. **e** PSTH of the response of the same cell to increasing concentrations of M3. **f** Plot of the concentration-response function of the responses shown in **e**. **g** PSTH of the response of neuron # 68 to ASW and increasing concentrations of M3. **h** Plot of the concentration-response function of the responses shown in **g**

Table 3. Responses of neurons to different chemical stimuli applied to the lateral flagellum of the antennule. Neurons ordered according to morphological type. *Column 1 (No.)*: identification number. *Column 2 (Type)*: morphological type. *Columns 3–17*: responses to different chemical stimuli, symbols as in Table 1; *ASW*, artificial sea water; *TM*, extract of TetraMarin in 1:10 dilution; *M1*, mixture 1 (taurine, betaine HCl, L-ascorbic acid, NH_4Cl, all at 1 mM); *M2*, mixture 2 (sucrose, nicotinic acid, AMP, tetramethylamine HCl, all at 1 m*M*); *M3*, mixture 3 (M1 + M2 + 1 m*M* L-proline); *Urine*, female urine diluted 1:10; *Tau*, 1 m*M* taurine; Bet, 1 m*M* betaine; Pro, 1 m*M* L-proline; *Asc*, 1 m*M* ascorbic acid; *Nic*, 1 m*M* nicotinic acid; *AMP*, 1 m*M* adenosine monophosphate; *NH4*, 1 m*M* NH_4Cl; *TMA*, 1 m*M* trimethylamine HCl; *Suc*, 1 m*M* sucrose

No.	Type	ASW	TM	M1	M2	M3	Urine	Tau	Bet	Pro	Asc	Nic	AMP	NH4	TMA	Suc
1	Motoneur. I	–	⬆	⬆	⬆			⇧	⇧	⇧	⬆	⇧	–	⇧	⇧	–
3	Motoneur. I	–	⬆⇧	⬆⇧	⇧⬆–			⇧– –	–	⇧– –	⇧–⇧	–	⇧⬆⇧	–	–	–
4	Motoneur. I?	–	–	⬆	⇧		⬆	–	–	–	–	–	–	–	–	–
5	Motoneur. I	⇧– –		⇧⬆⇧	⇧⬆⇧	⇧⬆⇧	⇧⇩⇧	⇧⬆⇧	⇧⇩–	–⇩⇧	⇧⇩⇧	⇧– –	⇧⇩⇧	⇧⇩–	⇧⬆–	⇧– –
6	Motoneur. I	–	–	⬆	⇧			⇧	–	⇧	–	–	⇧	–	–	–
9	Motoneur. I	–	⬆⬆–	⬆⇩–	⬆⬆–	⇧⬆–	⇧⇩–	⬆– –	⬆⬆⇧	⇧⬆–	⬆– –	⇧–	⇧⬆–	⇧–	⬆⬆⇧	–
2	desc. brain	–		⬆	⬆		–	⬆	–	⬆	⬆	⬆	⬆	–	⬆	–
8	desc. brain	–	⬆	⬆	⇧	⬆	–	⬆	⇧		⬆	⇧	–	–	–	
7	desc. eyest.	–	⇧	⬆	⬆	⇧	⇧	⬆	⇧	⇧	⇧	–	⇧		⬆	⬆

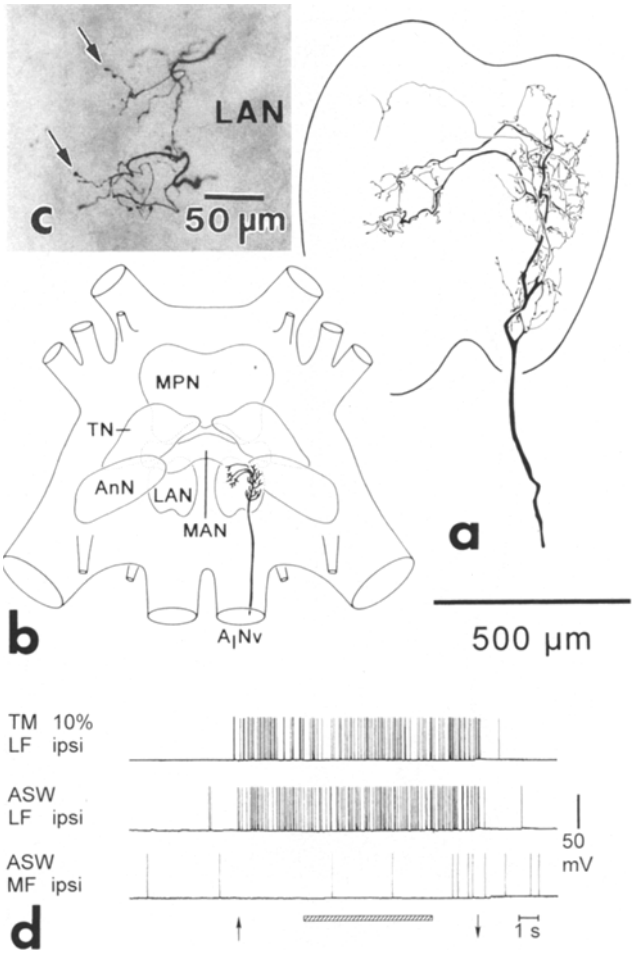

Fig. 4a–d Characterization of a mechanosensory antennular afferent (# 67) with arborizations confined to the LAN. **a** Reconstruction from serial horizontal vibratome sections. Note axon penetrating the lateral lobe of the LAN and arborizations crossing to the medial lobe. **b** Schematic representation of neuron position in the central brain. **c** LM micrograph of a horizontal vibratome section with biocytin-filled profiles in the medial lobe of the LAN. Note terminal boutons (*arrows*). **d** Traces of the response to stimulation of the LF with TetraMarin extract (*TM*) and *ASW* and to stimulation of the MF with ASW. *Hatched bar*, duration of chemical stimulus

Antennular sensory afferents

Three of the neurons, identified as antennular sensory afferents, had a thick (10–50 µm diameter) axon in the main antennular nerve (A_1Nv) and responded solely to mechanical stimulation (Tables 1, 2). One of these afferents (# 67) responded to mechanical stimulation of the lateral flagellum with tonic excitation and arborized exclusively in the lateral antennular neuropil (LAN) (Fig. 4). Target of the axon and area of main arborization was the lateral lobe of the LAN. The medial lobe also contained a small arbor arising from an anterior branch in the lateral lobe. The terminals of this afferent carried numerous boutons, about 1 µm in diameter.

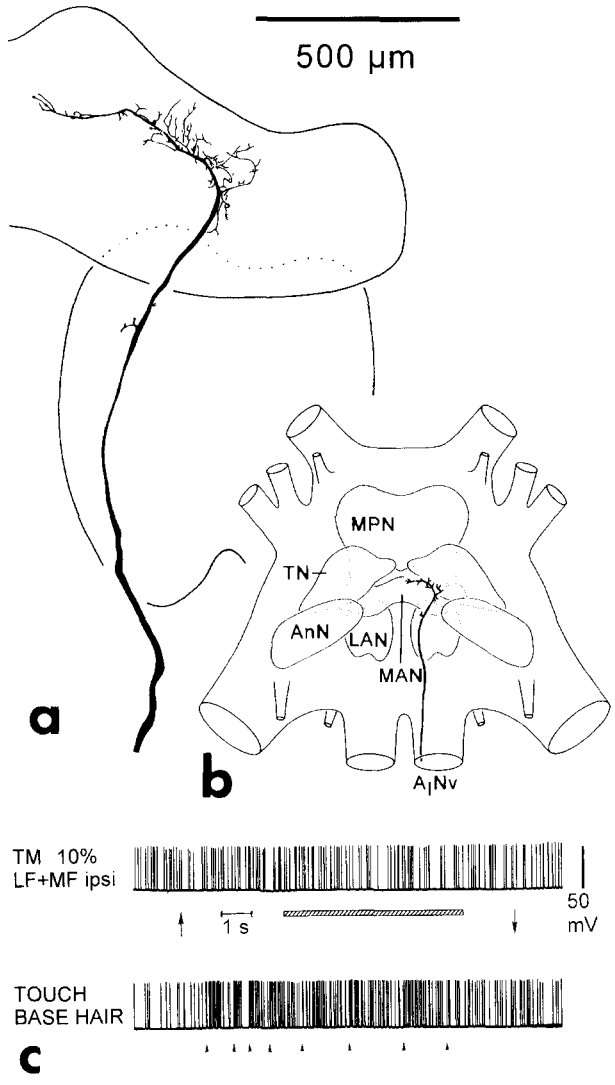

Fig. 5a–c Characterization of a mechanosensory antennular afferent (#68) with primary arborizations in the MAN and only minor branches in the LAN. **a** Reconstruction from serial horizontal vibratome sections. **b** Schematic representation of neuron position in the central brain. **c** Traces of the response to stimulation of the LF and MF with *TM* and to touching a hair sensillum at the base of the antennule. *Hatched bar*, duration of chemical stimulus

The other two afferents responded phasically to mechanical stimulation at the base of the antennule and arborized in the ipsilateral part of the median antennular neuropil (MAN) (Fig. 5). One (#68) responded exclusively to movement of one feathered hair on the 1st basal segment of the antennule (Fig. 5c) and the other (#66) to touch of the 3rd basal segment.

Antennular motoneurons

Twelve of the neurons, identified as motoneurons innervating muscles of the antennule, were ipsilateral and as a group arborized in the LAN, the MAN and the tegumentary neuropil (Table 1, Figs. 6–10). Only one neuron (#3) also arborized elsewhere, in this instance in the posterior of the median protocerebral neuropils (Fig. 6a, b). The somata were located in the dorsal or the lateral subcluster of the dorsal unpaired median cluster (dDUMC, lDUMC; Table 1, Fig. 2b). Among the morphologically characterized neurons antennular motoneurons were the only ones to be inhibited (all or in part) by chemical stimulation (Tables 2, 3, Figs. 6d, 7d, 8c). The 12 motoneurons were assigned to 3 types based on morphological criteria defined by Schmidt and Ache (1993).

Nine of the 12 cells equally innervated both lobes of the LAN and the MAN and to a lesser extent the tegumentary neuropil (TN), making them type I motoneurons. They varied in the fine pattern of branching, the localization and size of the somata and axons, as well as in physiological responsiveness (Figs. 6–8). The responses to chemosensory stimulation ranged from "simple" excitations, over "simple" inhibition to "complex" response profiles consisting of an inhibitory and one or two excitatory components. Three type I motoneurons did not respond to mechanical stimulation (of the lateral flagellum), all the others showed "simple" excitations at the beginning and/or the stop of the ASW flow. One of the 12 motoneurons had a dense arbor in the MAN, a smaller field of arborization in the TN and only few minor branches in the LAN and was thereby identified as type II motoneuron (Fig. 9). This motoneuron had no spontaneous activity and did not respond to mechanical stimulation, but was strongly depolarized and excited by chemical stimulation of the lateral flagellum. Two of the 12 motoneurons had rich arborizations in the LAN, but only minor branches in the MAN and none in the TN and were thereby identified as type III motoneurons (Fig. 10). One (#25) of these two responded only to the chemical stimulation of the lateral flagellum with a "complex" inhibition, while the other one (#58) was bimodal. In this motoneuron the response to the chemical stimulus was a "simple" strong excitation; to the mechanical stimulus the response was "complex" consisting of an initial inhibition characterized by a large IPSP and a subsequent excitation (Fig. 10d). The mechanosensory response varied considerably with the flagellum stimulated and the direction of the stimulus (start or stop of ASW flow) (Fig. 10d).

Projection neurons descending from the central brain

Seven of the neurons, identified as projection neurons descending from the central brain to the ventral cord, as a group arborized in the lateral and median antennular neuropils (LAN, MAN), in the antenna II and the tegumentary neuropils (AnN, TN), and in the anterior and the posterior median protocerebral neuropils (MPN) (Table 1, Figs. 11, 12). All but one of these

neurons (#63) arborized bilaterally. Their somata collectively occurred in the three subclusters (dorsal, lateral, median) of the dorsal unpaired median cluster and in the anterior cluster (Table 1, Figs. 2b, 11a). All showed a "simple" phasic or phasic-tonic excitation upon chemical stimulation (Figs. 11e, 12c). Five of these neurons also responded to mechanical stimulation, either with a "simple" excitation (Fig. 12c) or an excitation preceded or followed by an inhibition (Fig. 11e). Medial flagellum input mimicked that evoked by lateral flagellum, save for one neuron (neuron #56), in which chemical stimulation of the lateral flagellum was far more effective than chemical stimulation of the medial flagellum.

Projection neurons ascending from the central brain

Two of the neurons, identified as projection neurons ascending from the central brain to the eyestalk

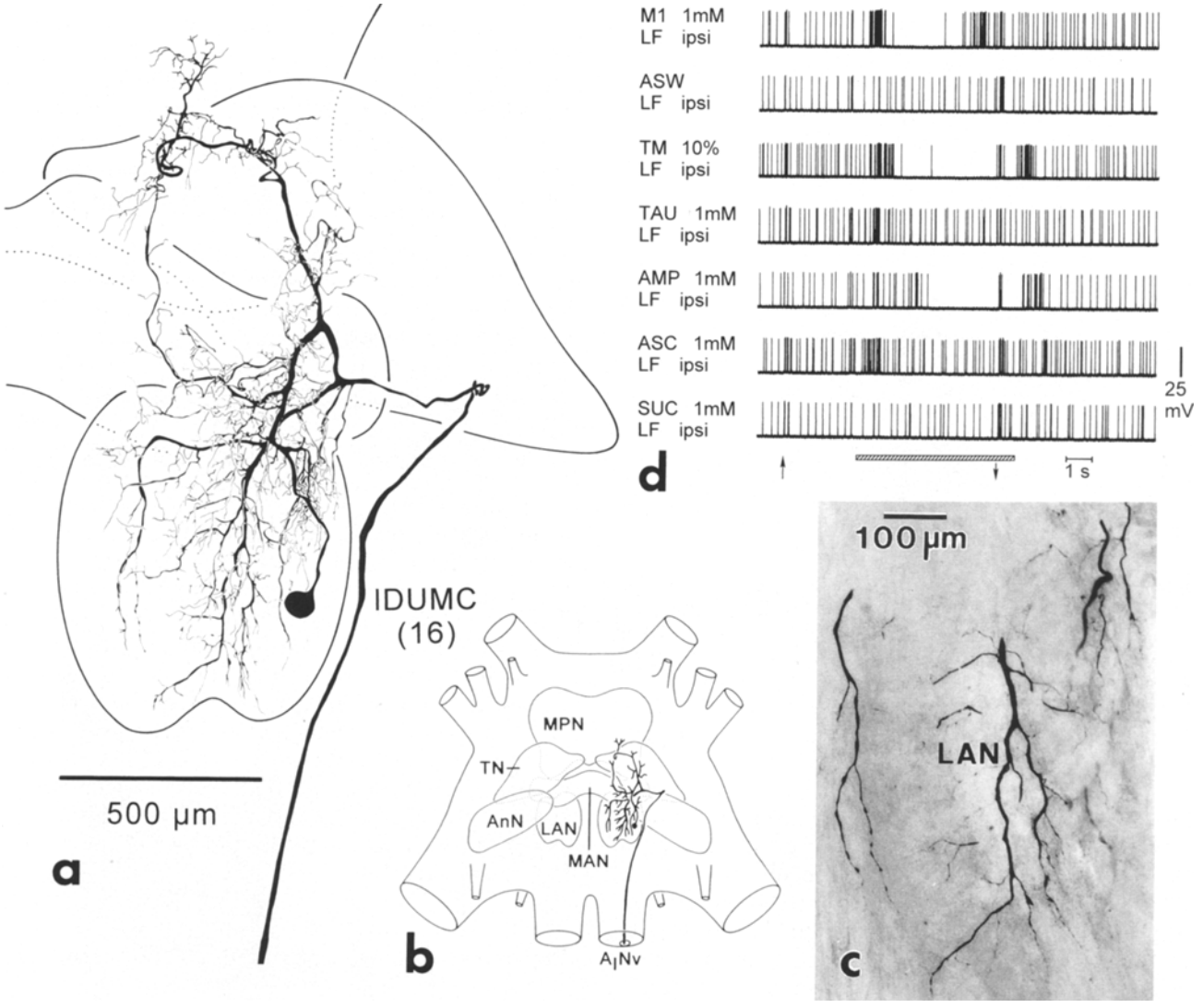

Fig. 6a–d Characterization of a type I antennular motoneuron (#3) with major arborizations in the LAN/MAN and the tegumentary neuropil (*TN*), and minor ones in the median protocerebral neuropils (*MPN*). **a** Reconstruction from serial horizontal vibratome sections. Soma located in the lateral subcluster of the dorsal unpaired median cluster (*IDUMC*). **b** Schematic representation of neuron position in the central brain. **c** LM micrograph of horizontal vibratome section with biocytin-filled profiles in the *LAN*. **d** Traces of the responses to stimulation of the LF with mixture 1 (*M1*), *ASW*, *TM*, *TAU*, adenosine monophosphate (*AMP*), ascorbic acid (*ASC*) and sucrose (*SUC*). Chemical stimulation elicited a complex response, consisting of an excitatory, an inhibitory and another excitatory phase or parts of this pattern. *Hatched bar*, duration of chemical stimulus

ganglia, had extensive arbors in the AnN and the median protocerebral neuropils (MPN), only minor branches in the TN and MAN, and somata of approximately the same size in the anterior subcluster of the medial cluster (aMC) (Table 1, Figs. 2b, 13). Only one of them (#59) arborized extensively in both lobes of the LAN and had contralateral arborizations in the posterior median protocerebral neuropil (Fig. 13). This neuron responded to mechanical stimulation of both flagella, but to chemical stimulation of only the medial flagellum. The other neuron (#26) lacked any branches in the LAN and responded to chemical but not mechanical, stimulation of the lateral flagellum.

Projection neurons descending from the eyestalk ganglia to the central brain

Two neurons, identified as projection neurons descending from the eyestalk ganglia to the central brain, were both strictly ipsilateral, and had terminals studded with boutons but had no other morphological or physiological similarities (Table 1, Figs. 14, 15). One neuron (#7) had very dense, extremely fine arborizations in both neuropils of the median protocerebrum (MPN) and some minor branches in the MAN. This neuron responded moderately to mechanical and vigorously to chemical stimulation of the lateral flagellum (Fig. 14). The other neuron (#19) had an extremely thick axon

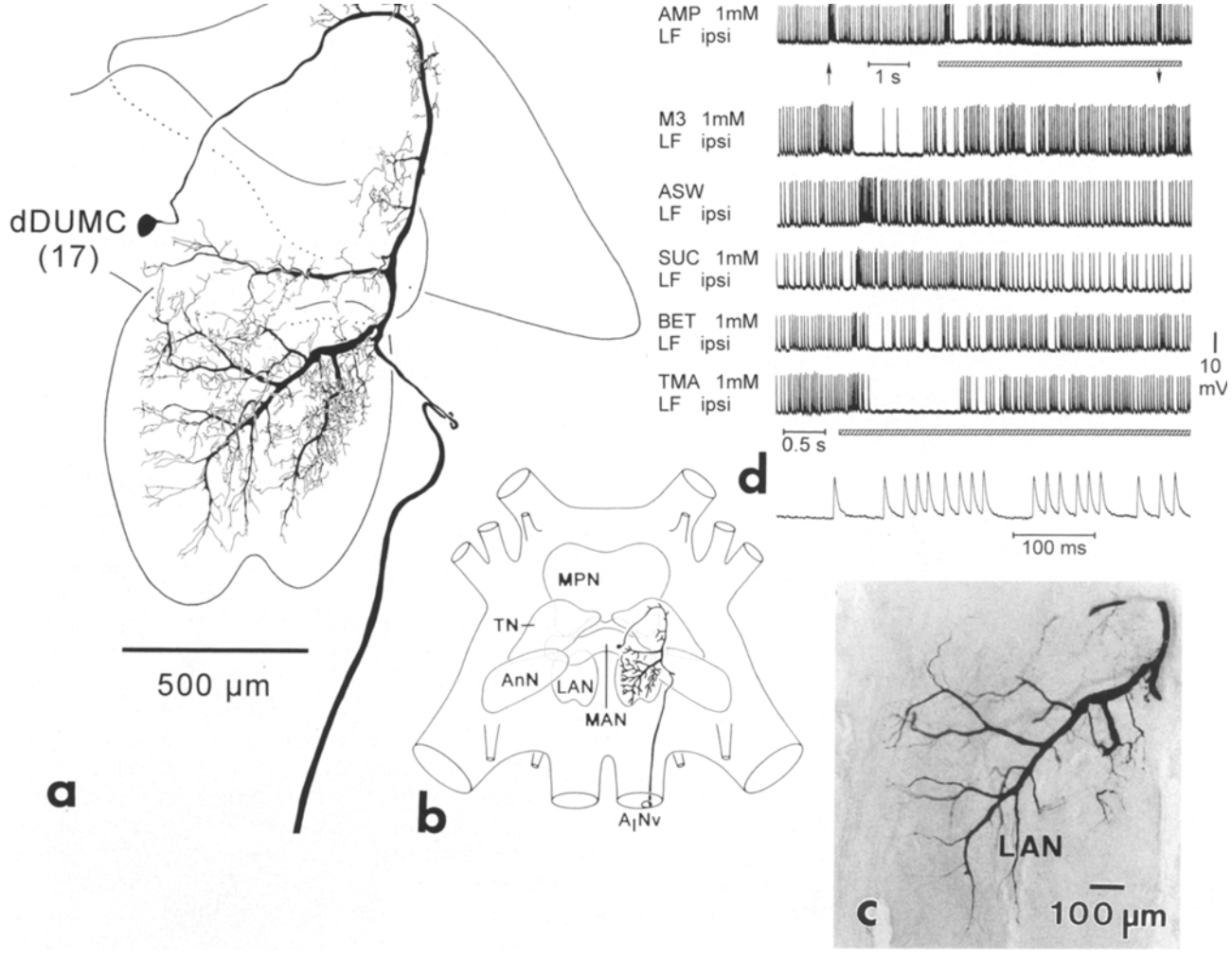

Fig. 7a–d Characterization of a type I antennular motoneuron (#5) with major arborizations in the LAN, one prominent neurite in the MAN and minor arborizations in the TN. **a** Reconstruction from serial horizontal vibratome sections. Soma located in the dorsal subcluster of the dorsal unpaired median cluster (*dDUMC*). **b** Schematic representation of neuron position in the central brain. **c** LM micrograph of horizontal vibratome section with biocytin-filled profiles in the *LAN*. **d** Traces of the response to stimulation of the LF with *AMP*, *MI*, *ASW*, *SUC*, betaine (*BET*), and trimethylamine HCl (*TMA*). Chemical stimulation elicited a complex response consisting of an excitatory, an inhibitory, and a subsequent excitatory phase, although parts of this pattern could be absent. *Hatched bar*, duration of chemical stimulus. *Bottom trace*, recording at expanded sweep reveals no synaptic activity during chemical stimulation

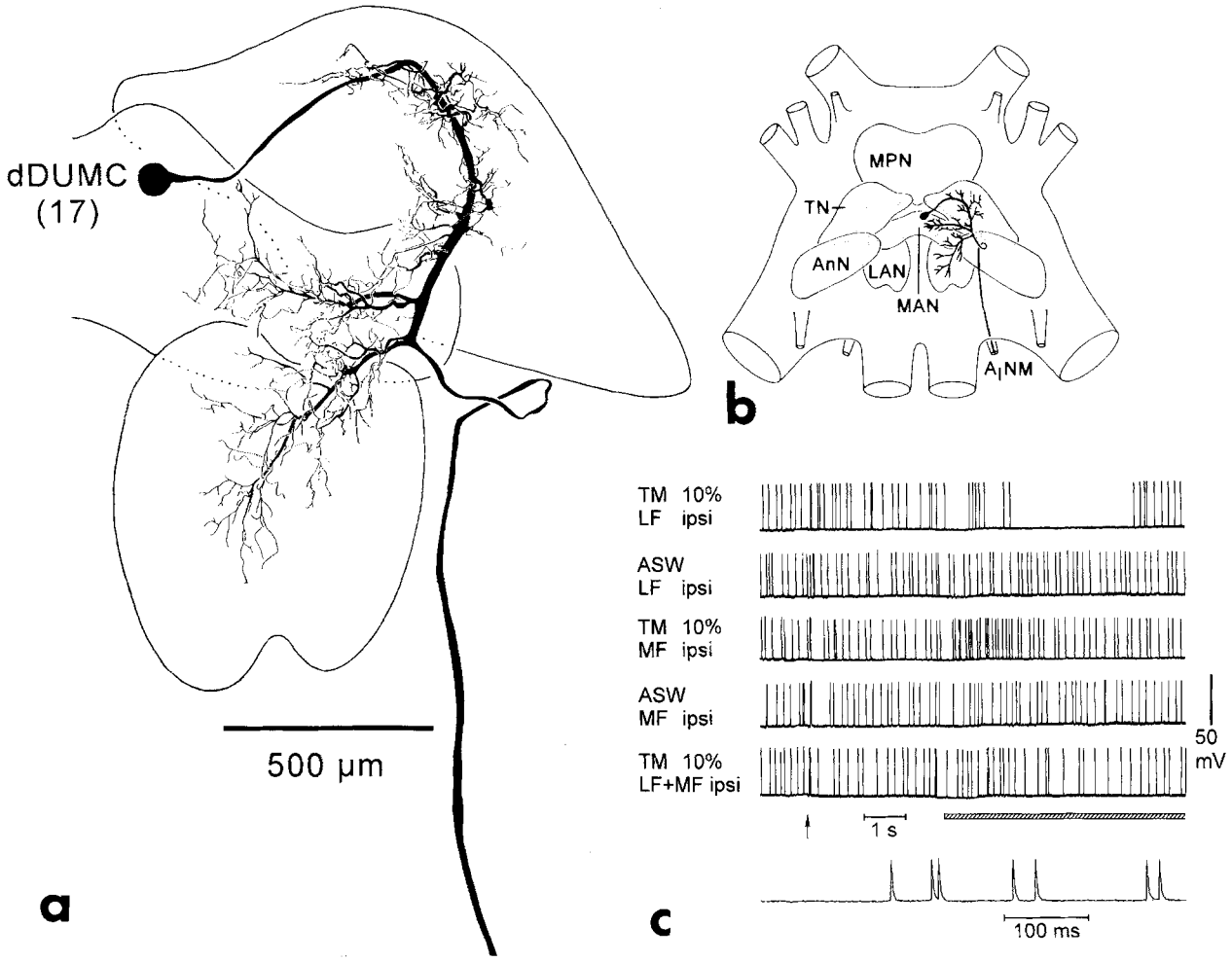

Fig. 8a–c Characterization of a type I antennular motoneuron (#64) with major arborizations in the LAN/MAN and in the TN. **a** Reconstruction from serial horizontal vibratome sections. Soma located in the dorsal subcluster of the dorsal unpaired median cluster (*dDUMC*). **b** Schematic representation of neuron position in the central brain. **c** Traces of responses to stimulation of the LF and the MF with *TM* and *ASW*, and to simultaneous stimulation of both flagella with TM. *Note*: LF stimulation elicited simple inhibition, MF stimulation elicited a small, simple excitation, but stimulation of both flagella failed to elicit any response. *Hatched bar*, duration of chemical stimulus. *Bottom trace*, recording at expanded sweep reveals no synaptic activity during chemical stimulation

(45 µm), its major arbor in the TN and only minor branches in the LAN, the MAN, the AnN and the neuropils of the median protocerebrum (MPN). This neuron responded slightly to chemical but not to mechanical stimulation of the lateral flagellum (Fig. 15).

Backfilling of projection neurons and motoneurons of eyestalk muscles

To determine how well our single neurons represented the connections of LAN and MAN, we backfilled the protocerebral tracts (PT; $n = 8$), the oesophageal connectives (OC; $n = 5$), and the oculomotor nerves (OCM; $n = 2$). The PT contained five clearly distinguishable groups of axons: (i) many thousand very thin axons of ascending projection neurons of the olfactory deutocerebrum constituting the olfactory globular tract; (ii) some thick axons of presumptive descending neurons of the eyestalk ganglia innervating the olfactory deutocerebrum; (iii) several hundred very thin axons of ascending projection neurons innervating the so-called "antennular glomeruli", small paired neuropils of the dorsal tritocerebrum, with globuli-type somata in the "dorsal unpaired globuli cell cluster", (iv) numerous mostly thick axons of neurons passing through the protocerebral bridge that connect the eyestalk ganglia of both sides, and (v) at least several hundred axons of other ascending neurons of the central brain and descending neurons of the eyestalk ganglia, among them all projection neurons with arborizations in the LAN and MAN.

Projection neurons of the latter type (v) arborized extensively in the ipsilateral TN and AnN of the tritocerebrum (Fig. 17a), in the entire MAN, in the ipsilateral LAN (Fig. 17c), in the ipsilateral deutocerebral

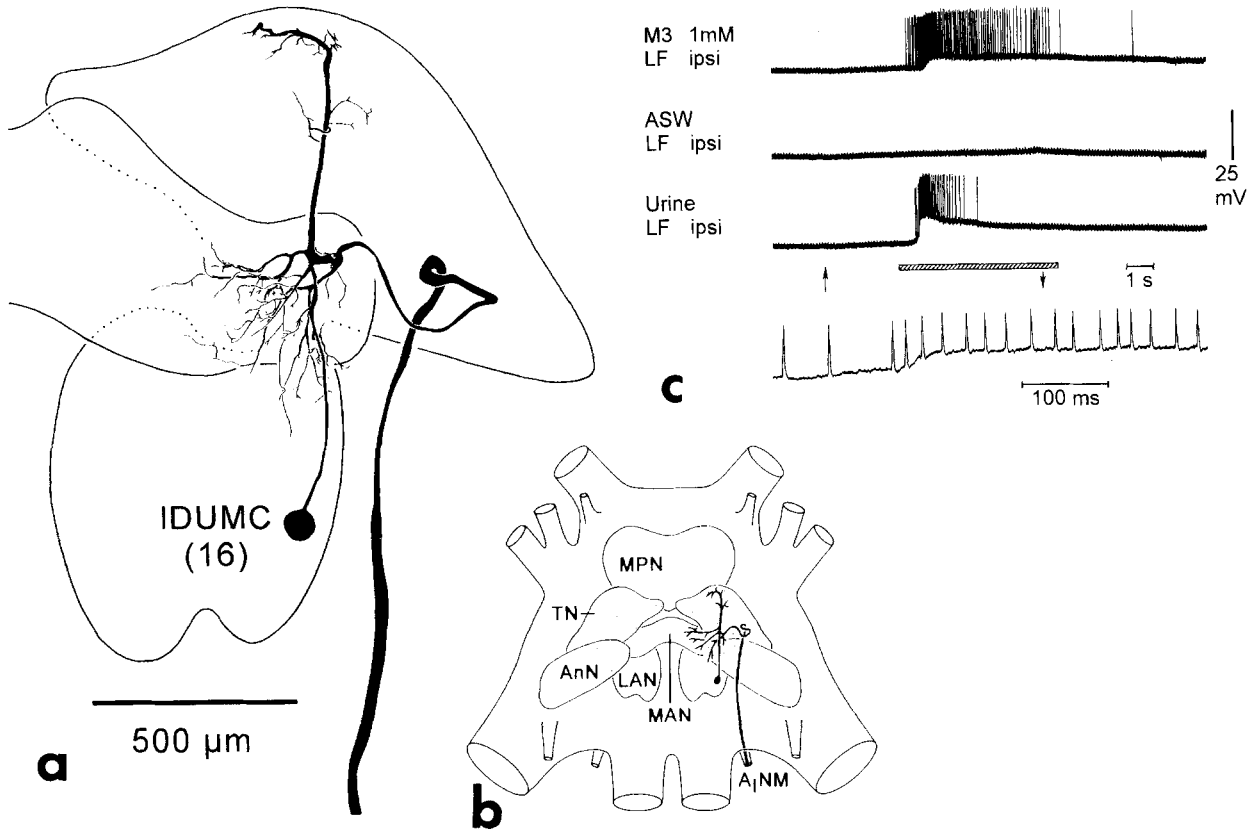

Fig. 9a–c Characterization of a type II antennular motoneuron (#10) with major arborizations in the MAN, some arborizations in the TN and only very minor branches in the LAN. **a** Reconstruction from serial horizontal vibratome sections. Note absence of fine terminals branches indicating incomplete fill. Soma located in the lateral subcluster of the dorsal unpaired median cluster (*IDUMC*). **b** Schematic representation of neuron position in the central brain. **c** Traces of responses to stimulation of the LF with *M3*, *ASW*, and *Urine*. Chemical stimulation elicited a strong, long-lasting phasic-tonic increase in discharge and summed EPSP. *Hatched bar*, duration of chemical stimulus. *Bottom trace*, recording at expanded sweep reveals a long lasting EPSP

commissure neuropil (DCN), and in the ipsi- and contralateral MPNs. Minor arborizations were present in the contralateral tritocerebral neuropils, in the contralateral LAN and in the central body. This group of neurons contained about 660 ascending projection neurons of the central brain (per hemibrain) as indicated by the total number of somata distributed over 5 different soma clusters. Most somata of ascending projection neurons were located in the dDUMC (ca. 115), the aMC (ca. 185), and the AC (ca. 150).

Most arborizations in the LAN arose from thicker fibers running along the lateral edges of both lobes and were connected to somata in the aMC (Fig. 17c). In the aMC the backfilled somata formed two distinct groups: a dorsal group consisting of about 115 somata and a group of about 70 somata scattered in the ventral part. All somata in the dorsal group and some of the ventral group apparently were connected to arborizations in the LAN. Thus, there are at least 120 ascending neurons of the central brain with major arborizations in the LAN per hemibrain. These neurons further arborize in the ipsilateral neuropils of the tritocerebrum, in the MAN and the median protocerebrum.

Clear subsets of neurons could not be identified in the OC, suggesting that the labeled neurons represent a very heterogeneous population of descending brain neurons and ascending neurons of the ventral cord. As a group these neurons arborized most densely in the ipsilateral TN (Fig. 17b). Major arborizations also occurred in the ipsilateral AnN (Fig. 17b), LAN (Fig. 17d), "Antennular Glomeruli", "Antennal Glomeruli" (another pair of neuropils in the dorsal tritocerebrum), and MPN, as well as in the ipsi- and the contralateral MAN. Minor arborizations occurred in the ipsilateral neuropils of the olfactory deutocerebrum and in the contralateral TN, AnN, LAN, and MPN. The innervation of the LAN arose predominantly from very thick fibers that penetrated both lobes centrally and sent fine terminals peripherally (Fig. 17d). It was not possible to determine a connection between the thick fibers and labeled somata. Among the whole population of projection neurons with axon in the OC, about 716 in each hemibrain had their soma in the central brain and were thus characterized as projection neurns descending from the central brain to the ventral cord. Filled somata of descending projection neurons

were located in 6 soma clusters (DLC, DUMC, aMC, VPALC, VUMC, AC), among which the AC contained by far the highest number of labeled somata (ca. 570 per hemibrain).

Backfilling the PT maximally stained about 30 axons in the OC, while backfilling a connective stained a maximum of about 12 axons in the PTs. Thus, some projection neurons pass through the central brain and may represent projection neurons that ascend from the ventral cord to the eyestalk ganglia and/or projection neurons descending from the eyestalk ganglia to the ventral cord.

The backfills of the OCM labeled 35–37 motoneurons, most of which had somata in the ventral part of the aMC, where they formed a clearly defined subcluster. One stained soma occurred in the ipsilateral VUMC. All arborizations were strictly ipsilateral. Most densely innervated were the TN, the MAN, and the posterior MPN, minor arborizations occurred in the LAN and the anterior MPN.

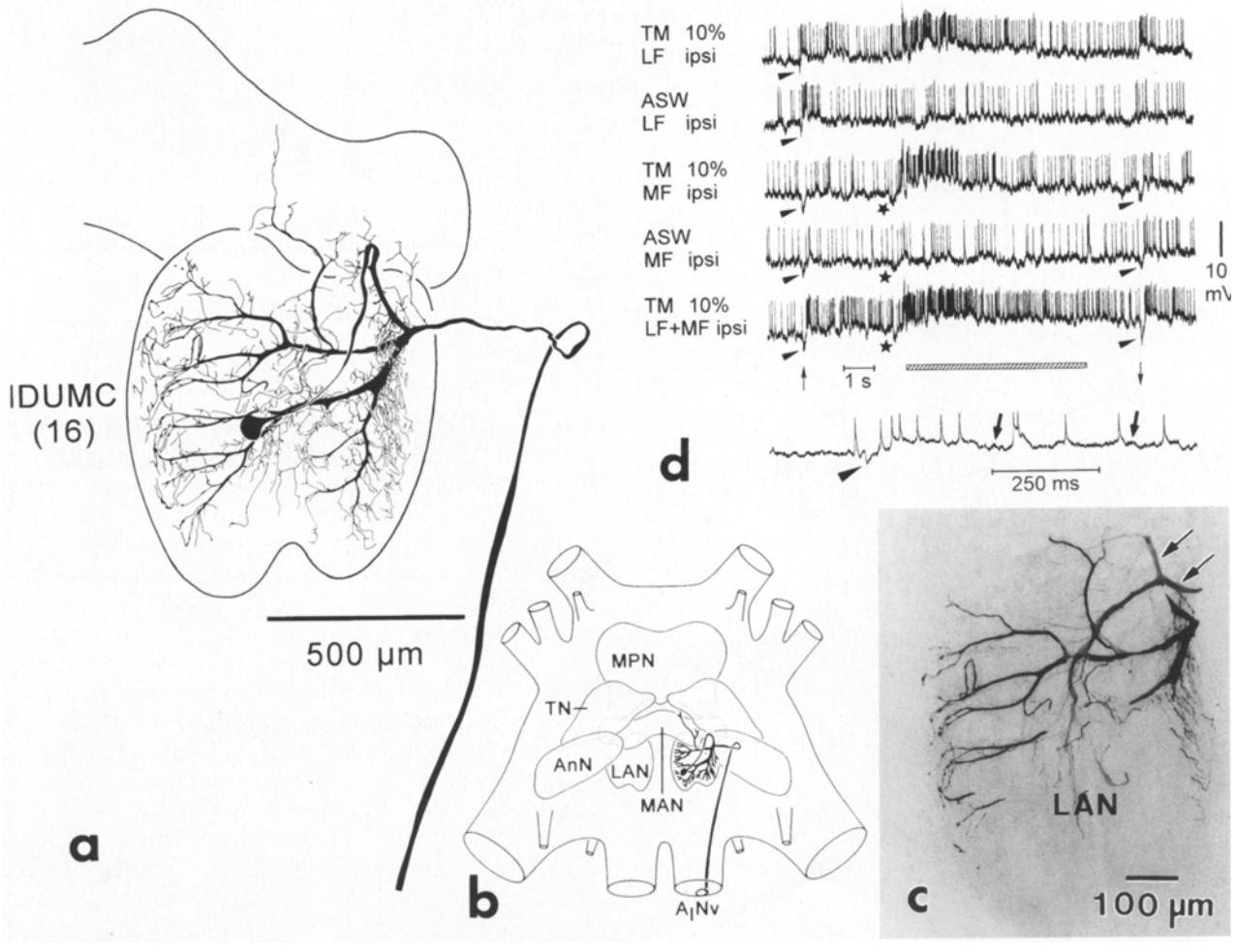

Fig. 10a–d Characterization of a type III antennular motoneuron (#58) with prominent arborizations in the LAN penetrating the whole neuropil, very minor arborizations in the MAN and no branches in the TN. **a** Reconstruction from serial horizontal vibratome sections. Localization of soma in the lateral subcluster of the dorsal unpaired median cluster (*IDUMC*). **b** Schematic representation of neuron position in the central brain. **c** LM micrograph of horizontal vibratome section with biocytin-filled profiles in the LAN. Note the lightly-filled neurite of another neuron (*arrows*), suggestive of dye coupling. **d** Traces of responses to stimulation of the LF and MF with *TM* and *ASW*, and to simultaneous stimulation of both flagella with TM. Chemical stimulation elicited increases in discharge and compound EPSP. The response to simultaneous stimulation of both flagella was additive. Mechanical stimulation elicited a complex response consisting of a large IPSP (*arrowheads*) and a longer-lasting increase in discharge and succession of short EPSPs. Note the IPSP was longer for MF stimulation, while excitation was more prominent for LF stimulation. Simultaneous stimulation of both flagella was additive, yielding a long IPSP plus long-lasting excitation. Note that MF stimulation elicits small IPSPs before onset of the chemical stimulus (*stars*). *Hatched bars*, duration of chemical stimulus. *Bottom trace*, recording at expanded sweep during mechanical stimulation of MF reveals an IPSP (*arrowhead*) at the beginning and repetitive EPSPs (*arrows*) during excitatory phase of response

Discussion

Functional properties of the LAN and MAN

LAN: Our physiological results show that the LAN is a primary sensory neuropil integrating mechano- and chemosensory antennular input as well as a lower motor center for antennular reflexes (Fig. 18). All neurons in the present study with arborizations in the LAN responded to antennular sensory input. Similarly, Glantz et al. (1981) showed that in crayfish 35 of 37 descending projection neurons that arborized in the LAN received afferent input from the corresponding antennule. Most of the neurons in the present study with arborizations in the LAN were bimodal and

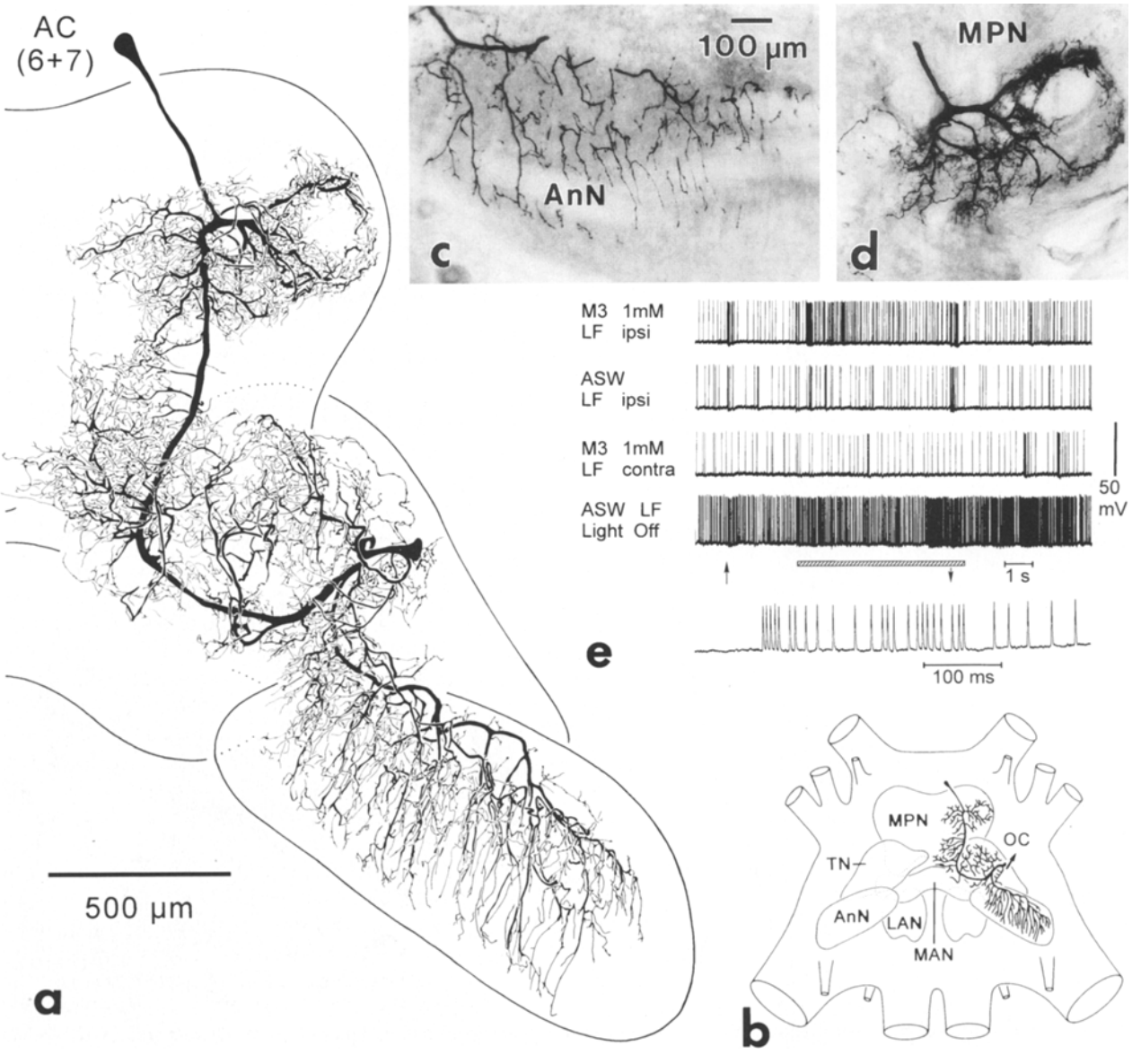

Fig. 11a–e Characterization of a descending projection neuron of the central brain (#12) with prominent arborizations in the antennal neuropil (AnN) and in both median protocerebral neuropils (MPN), in particular the anterior one, some additional arborizations in the TN and in the MAN. **a** Reconstruction from serial horizontal vibratome sections. Soma located in anterior cluster (*AC*). **b** Schematic representation of neuron position in the central brain. Axon leaving the central brain via oesophageal connective (*OC*). **c, d** LM micrographs of horizontal vibratome sections with biocytin-filled profiles, **c** in the *AnN* and **d** in the *MPN*. **e** Traces of responses to stimulation of the ipsilateral LF with *M3* and *ASW*, the contralateral LF with *M3* and the LF with *ASW* during reduced ambient light. Chemical stimulation elicited a long-lasting phasic-tonic increase in discharge. Mechanical stimulation elicited a brief, phasic increase in discharge. Note that reduced light increased the spontaneous activity of the neuron dramatically. *Hatched bar*, duration of chemical stimulus. *Bottom trace*, recording at expanded sweep reveals no synaptic activity during chemical stimulation

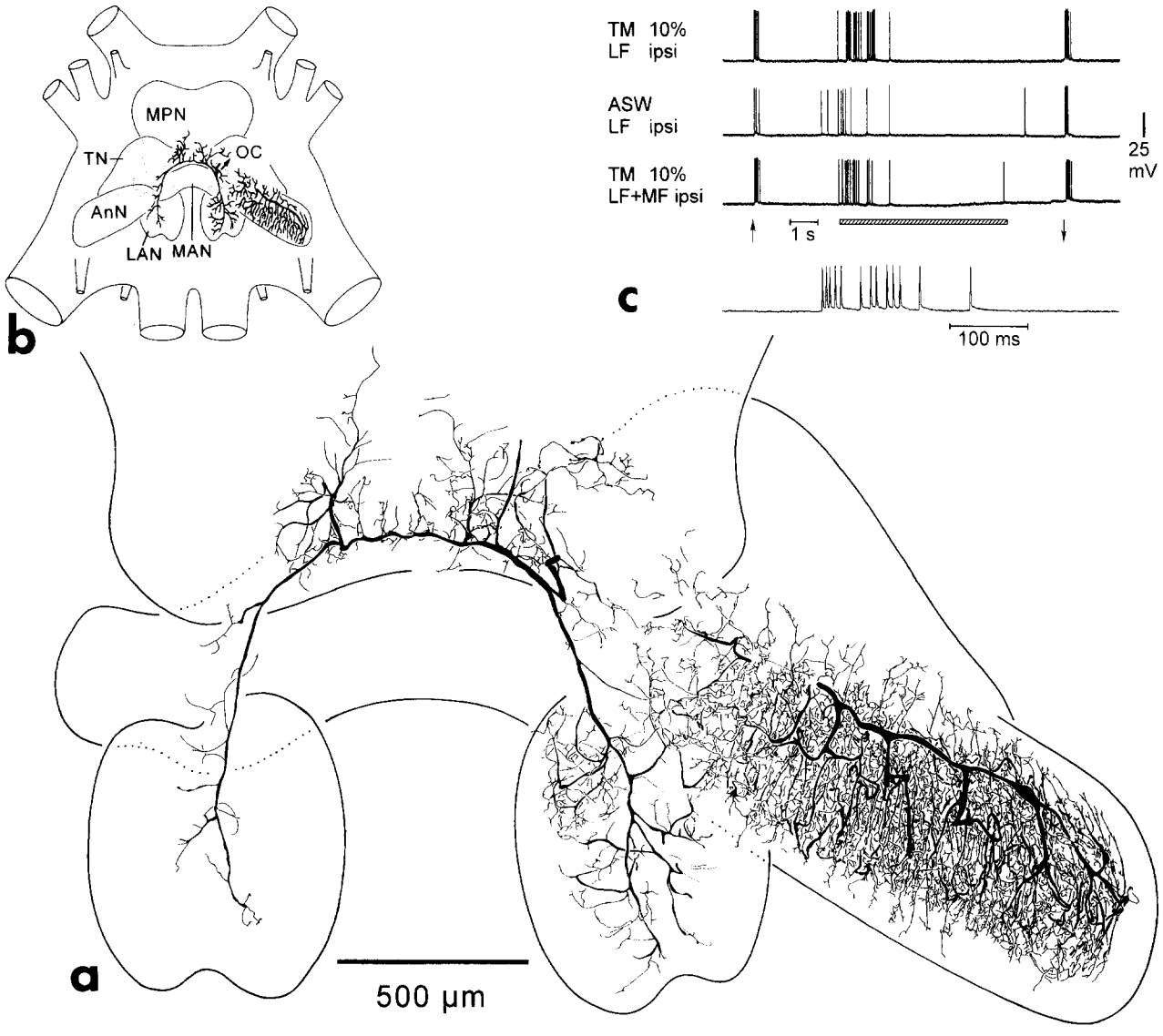

Fig. 12a–c Characterization of a descending projection neuron of the central brain (#24) with prominent arborizations in the ipsilateral AnN, less dense arbors in the ispilateral LAN and in both parts of the MAN and some additional arborizations in the contralateral LAN and in the MPN. **a** Reconstruction from serial horizontal vibratome sections. Soma and axon missing due to loss of sections. **b** Schematic representation of neuron position in the central brain. Most likely axon leaves the central brain via the OC. **c** Traces of responses to stimulation of the LF with *TM* and *ASW* and simultaneous stimulation of both flagella with *TM*. Chemical stimulation elicited a simple, brief increase in discharge. Mechanical stimulation elicited a similar response. Simultaneous mechanical, but not chemical, stimulation of both flagella elicited an additive response. *Hatched bar*, duration of chemical stimulus. *Bottom trace*, recording during mechanical stimulation at a faster sweep reveals no synaptic activity

exhibited complex responses, often responding in an opposite manner to the two modalities. The only afferent in our study that arborized in the LAN responded with a tonic excitation to the ASW flow, whereas all "LAN neurons" (projection- and motoneurons) responded phasically to the onset and/or end of the ASW flow, indicating that the afferent signal is differentially integrated, even though many connections between the sensory afferents and higher-order neurons appear to be monosynaptic (present study; Glantz et al. 1981). So far only one local interneuron has been identified in the central brain with arborizations in the LAN (Arbas et al. 1988: cell #13), suggesting that very few such neurons exist in the LAN that could form polysynaptic pathways between the sensory afferents and the projection- or motoneurons. Also, our backfill data show that the soma cluster most closely associated with the LAN (the dorsal part of the aMC) contains predominantly somata of ascending projection neurons, not local interneurons. All interneurons or motoneurons innervating the LAN arborize in both lobes (Hamilton and Ache 1983; Tautz et al. 1986; Tautz 1987; Arbas et al. 1988; Derby and Blaustein 1988; this study), allowing for input from both flagella due to the preferential

termination of medial flagella afferents in the medial lobe and of lateral flagellum afferents in the lateral lobe of the LAN (Schmidt et al. 1992). In agreement with this high level of connectivity between the two lobes of the LAN, we did not find a single neuron that responded exclusively to the stimulation of one flagellum (see also Derby et al. 1985), and we often found additive responses to simultaneous bilateral stimulation. All

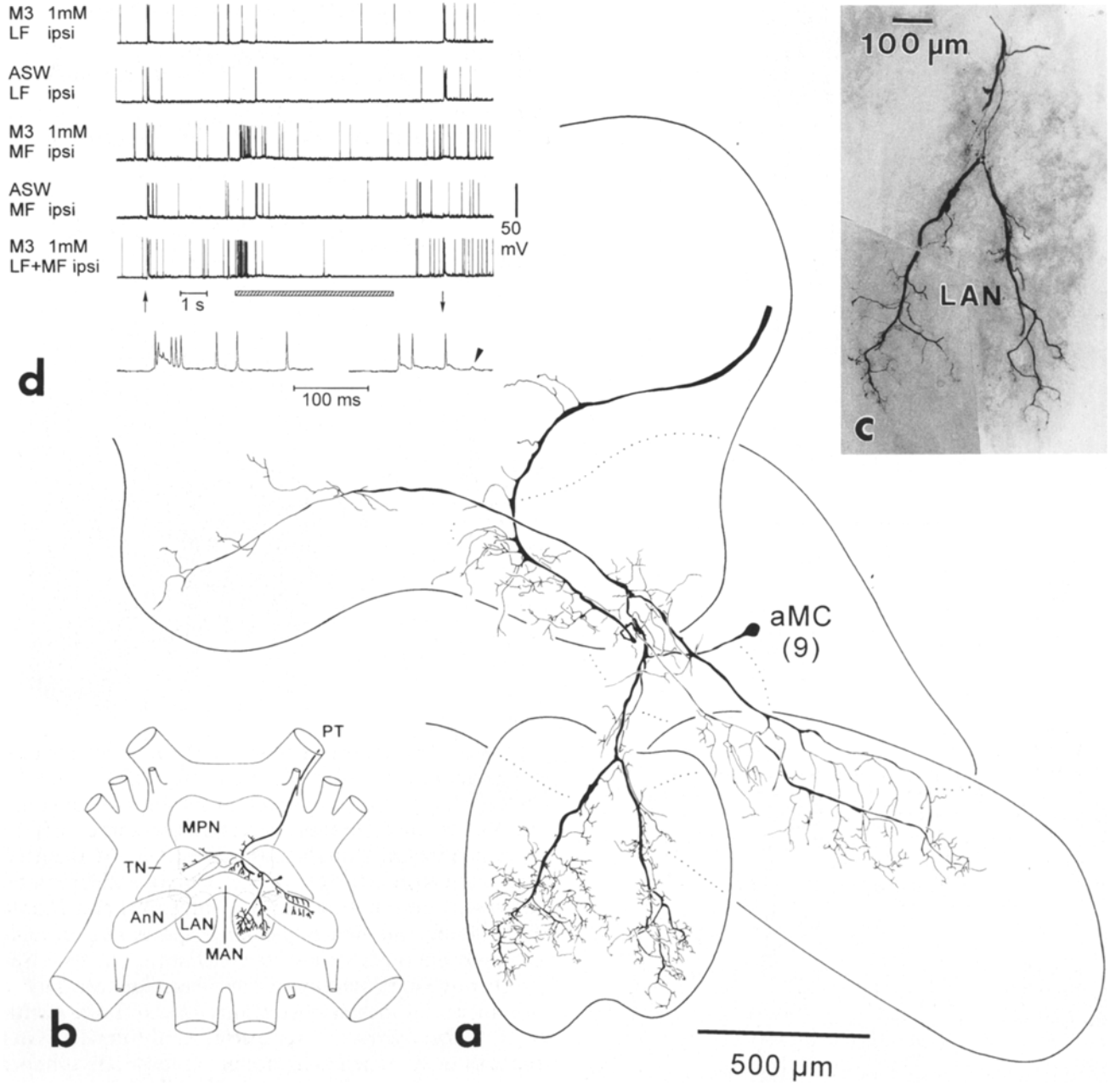

Fig. 13a–d Characterization of an ascending projection neuron of the central brain (#59) with prominent arborizations in the LAN, less dense arbor in the AnN and the ipsilateral MPN, some additional arborizations in the contralateral MPN, in the TN and the MAN). **a** Reconstruction from serial horizontal vibratome sections. Soma located in the anterior subcluster of the medial cluster (*aMC*). **b** Schematic representation of neuron position in the central brain. Axon leaving the central brain via protocerebral tract (*PT*). **c** LM micrograph of horizontal vibratome section with biocytin-filled profiles in the *LAN*. Note dense arbors in both lobes of the LAN. **d** Traces of responses to stimulation of the LF and MF with *M3* and *ASW*, and of simultaneous stimulation of both flagella with *M3*. MF stimulation elicited simple short excitation (increase in spiking). Mechanically stimulating the LF elicited short phasic mechanosensory responses of similar magnitude, while stimulating the MF only elicited a response at the onset. *Hatched bar*, duration of chemical stimulus. *Bottom trace*, recording at expanded sweep during chemical (*left*) and mechanical (*right*) stimulation of the MF reveals small EPSPs (*arrowhead*)

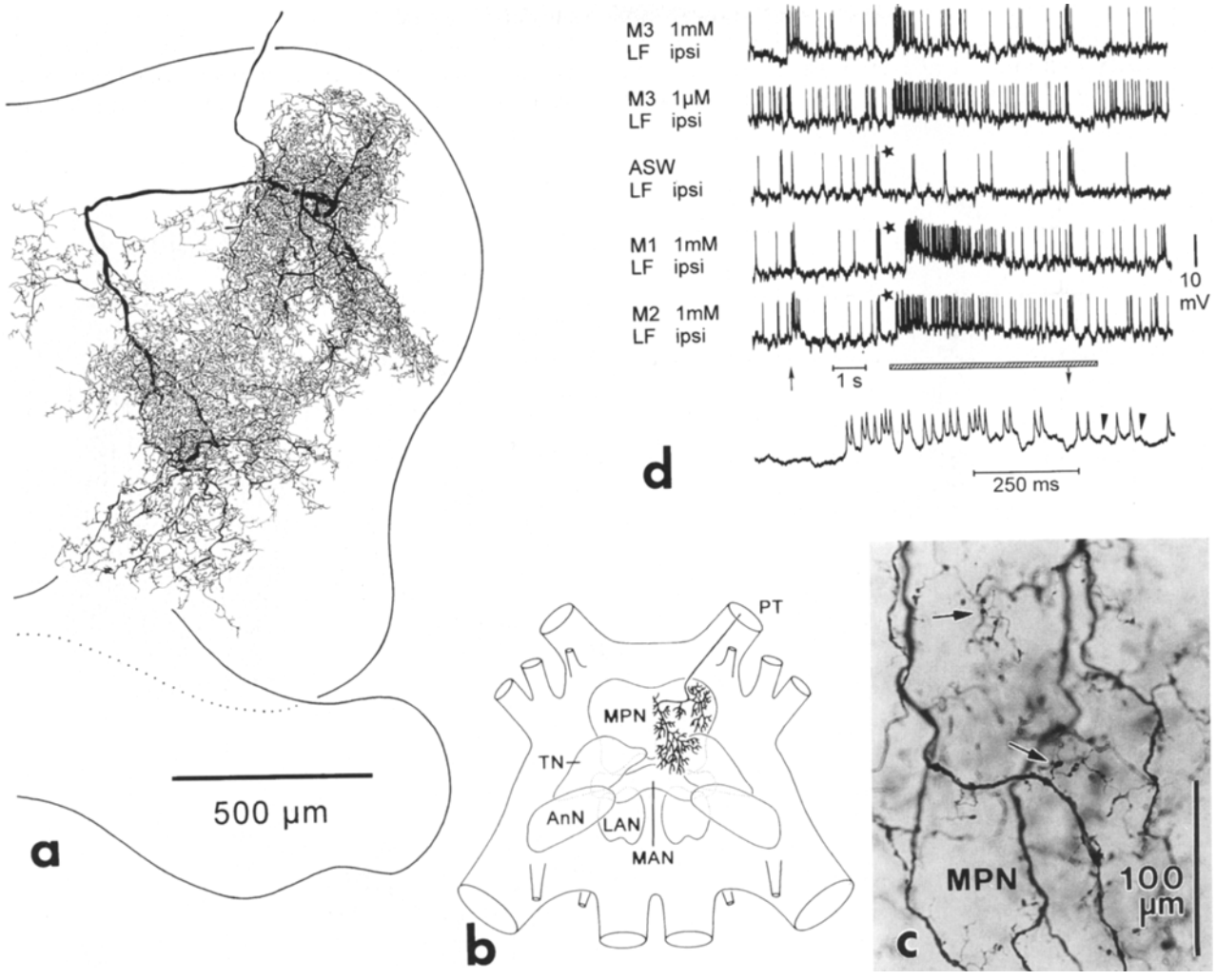

Fig. 14a–d Characterization of a descending projection neuron of the eyestalk (#7) with prominent and dense arborizations in both neuropils of the MPN and very sparse branches in the MAN. **a** Reconstruction from serial horizontal vibratome sections. **b** Schematic representation of neuron position in the central brain. Axon entering the central brain via protocerebral tract (*PT*). **c** LM micrograph of horizontal vibratome section with biocytin-filled profiles in the posterior median protocerebral neuropil (*MPN*). Note very fine terminal arborizations bearing numerous boutons (*arrows*). **d** Traces of responses to stimulation of the LF with *M1*, *M2*, *M3*, and *ASW*. Chemical stimulation elicited simple, prolonged phasic-tonic increases in discharge plus a compound EPSP. Mechanical stimulation elicited short phasic increases in discharge plus a compound EPSP. The small mechanical stimuli induced by switching between ASW and stimulus solution (*stars*) also elicited a brief response. *Hatched bar*, duration of chemical stimulus. *Bottom trace*, recording during chemical stimulation at expanded sweep speed reveals small EPSPs (*arrowheads*) riding on a compound depolarization

antennular motoneurons that we characterized in this study arborized in the LAN – some of them almost exclusively (type III) – and responded to antennular sensory input. This clearly corroborates our previous conclusion from biocytin backfills showing extensive overlap in the arborizations of antennular mechano- and chemosensory afferents and motoneurons, that the LAN is a substrate for antennular sensory-motor coupling and thus serves as lower motor center of the antennule (Schmidt and Ache 1992, 1993). Most likely local antennular reflexes to mechanical and/or chemical stimulation of the antennule (Maynard and Dingle 1963; Snow 1973) are primarily patterned in this neuropil.

MAN: Our physiological results suggest that the MAN is a primary sensory neuropil integrating mechanosensory – especially statocyst – and chemosensory antennular input, as well as a lower motor center of antennule and eyestalks (Fig. 18). Our present physiological results confirm morphological evidence (Schmidt et al. 1992) that the MAN receives and integrates mechano-and chemosensory input from both flagella of the antennule; neurons with arborizations in the MAN but not in the LAN (neurons #26, 56, 62) responded to chemostimulation, and in one instance mechanostimulation, of the flagella. The dominant input to the MAN, however, appears to be provided by mechanoreceptors at the base of the

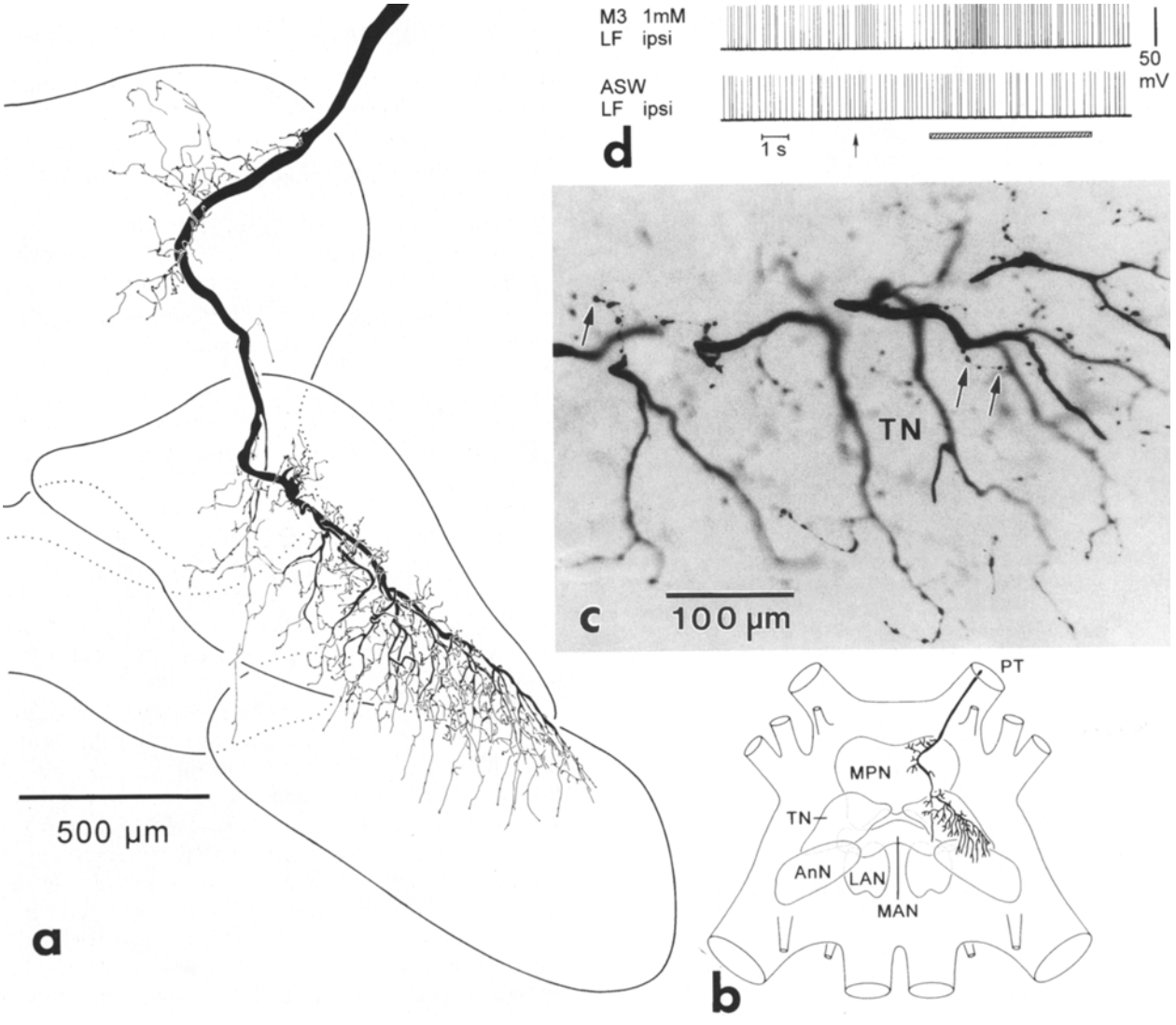

Fig. 15a–d Characterization of a descending projection neuron of the eyestalk (#19) with prominent arborizations in the TN, some additional arborizations in the AnN and the MPN and very minor branches in the MAN. **a** Reconstruction from serial horizontal vibratome sections. **b** Schematic representation of neuron position in the central brain. Axon entering the central brain via protocerebral tract (*PT*). **c** LM micrograph of horizontal vibratome section with biocytin-filled profiles in the *TN*. Note very fine terminal arborizations bearing numerous boutons (*arrows*). **d** Traces of responses to stimulation of the LF with *M3* and *ASW*. Chemical stimulation elicited a weak, brief increase in discharge. *Hatched bar*, duration of chemical stimulus

antennule. Afferents of statocyst and other mechanosensory hairs on the antennular base project to and apparently arborize exclusively in the MAN (Sandeman and Okajima 1973; Yoshino et al. 1983; Roye 1986; this study: neurons #66, 68). Many local interneurons (Nakagawa and Hisada 1991, 1992) and descending projection neurons of the central brain (Fraser 1974; Fraser and Sandeman 1975; Nakagawa and Hisada 1989, 1990) that respond to statocyst stimulation also arborize in the MAN. Statocyst input to the MAN feeds into several motor systems. One of these motor systems is comprised of the antennular motoneurons, all but one (neuron #10) of which we show have prominent arborizations in the MAN. Since statocyst stimulation induces reflexive compensatory movements of the antennule (Roye 1975), the MAN presumably serves as the lower antennular motor center driving this reflex. A second motor system is comprised of the motoneurons innervating the eyestalk muscles. We show that the motoneurons of the eyestalk muscles arborize extensively in the MAN as well as in the TN and the neuropils of the median protocerebrum, similar to the situation in crab (*Scylla serrata*: Sandeman and Okajima 1973) and crayfish (*Procambarus clarkii*: Mellon 1977). Eyestalk motoneurons receive some statocyst input via monosynaptic connections (e.g. Silvey and Sandeman 1976;

see review Neil 1982). Since the arborizations of the statocyst afferents and the eyestalk motoneurons only overlap in the MAN, the MAN presumably also represents the motor center driving compensatory eye movements in response to gravitational stimuli (see review Neil 1982).

Functional division of the deutocerebrum

Four lines of evidence suggest that the antennular sensory input to the LAN and MAN is functionally distinct from that going to the OL (see accompanying paper). First, is the nature of the chemosensory input. Although so far no obvious difference in the response properties of the olfactory and non-olfactory chemosensory sensilla on the antennule have been found (e.g. Fuzessery 1978; Spencer 1986; Tierney et al. 1988; Michel et al. 1993), the two inputs target different deutocerebral neuropils. Given that the olfactory afferents project exclusively to the OL and presumptive non-olfactory chemosensory afferents from both antennular flagella project predominantly to the LAN (Schmidt and Ache 1992), "LAN/MAN neurons" should receive non-olfactory chemosensory input from both flagella, while "OL neurons" should receive olfactory input only from the lateral flagellum. Seven neurons that arborized (#64, 58, 63, 59) or were recorded in the LAN/MAN (#43, 48, 57) and 18 neurons that arborized or were recorded in the OL (see accompanying paper) support this prediction; all "LAN/MAN neurons" received chemosensory input from the medial, and except one (#59), from the lateral flagellum, whereas of the 18 "OL neurons" (see accompanying paper) only one received chemosensory input from the medial flagellum and all received chemosensory input from the lateral flagellum.

Second, is the nature of the mechanosensory input. Mechanosensory afferents from the flagella and the basal segments of the antennule project to the LAN and the MAN, respectively (Sandeman and Okajima 1973; Yoshino et al. 1983; Roye 1986; Schmidt et al. 1992), while the OL is innervated by relatively few presumptive mechanosensory afferents of unknown antennular origin (Schmidt and Ache 1992). This innervation pattern suggests that integration of mechanosensory input from the antennule predominantly is the domain of the LAN/MAN pathway. We show that whereas 70% (21 of 30) of the LAN/MAN neurons respond to mechanical stimulation of the

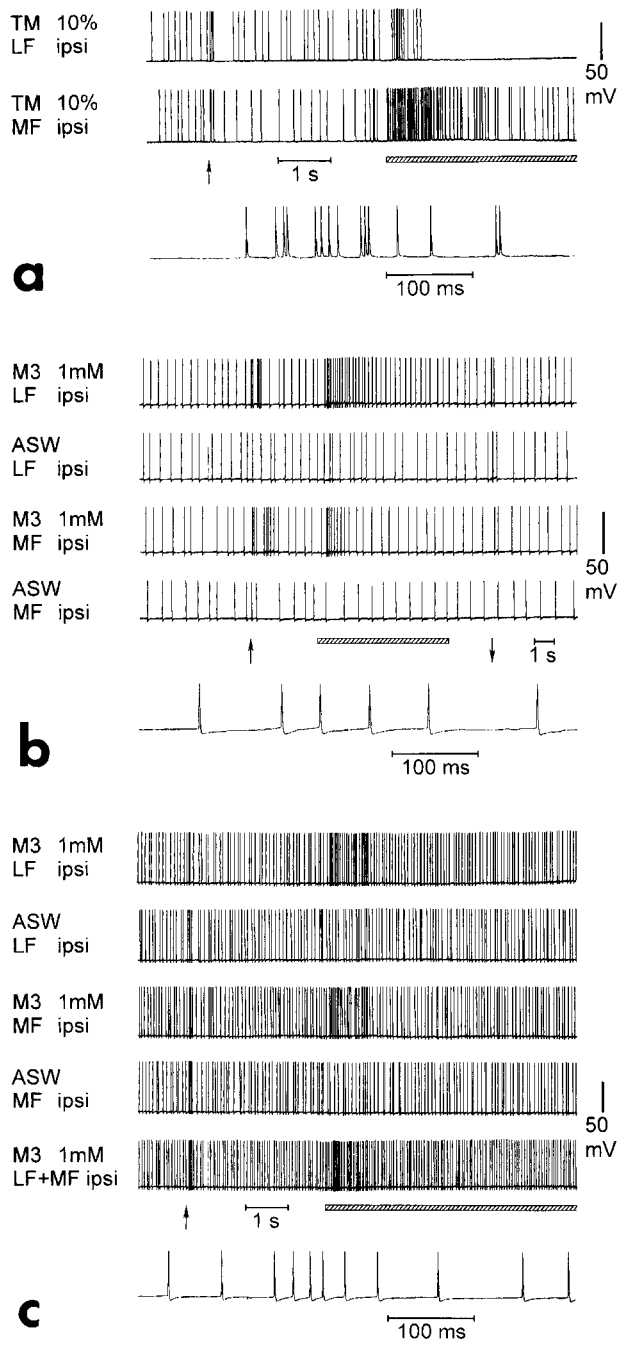

Fig. 16a–c Responses of neurons recorded in the LAN to stimulation of both antennular flagella. **a** Responses of neuron 43 to *TM*. The responses to chemical stimulation were flagellum-specific; LF stimulation caused a complex response consisting of a short, initial excitation (increase in spiking) and a subsequent prolonged inhibition (cessation of spiking), whereas MF stimulation caused a simple, prolonged phasic-tonic response. Similarly, mechanical stimulation of LF elicited a complex response consisting of a short excitation and a little longer inhibition, whereas MF stimulation gave a short phasic excitation. **b** Response of neuron 57 to *M3* and *ASW*. Chemical stimulation elicited a phasic-tonic excitation that lasted considerably longer and was stronger for LF stimulation. Mechanical stimulation elicited weak excitation. **c** Responses of neuron 63 to *M3* and *ASW*. Chemical stimulation of either flagellum elicited brief increases in discharge. Mechanical stimulation of either flagellum elicited brief increases in discharge followed by brief decreases in discharge. *Hatched bar*, duration of chemical stimulus. *Bottom trace* in each instance shows the absence of synaptic activity during chemical stimulation at fast sweep speeds

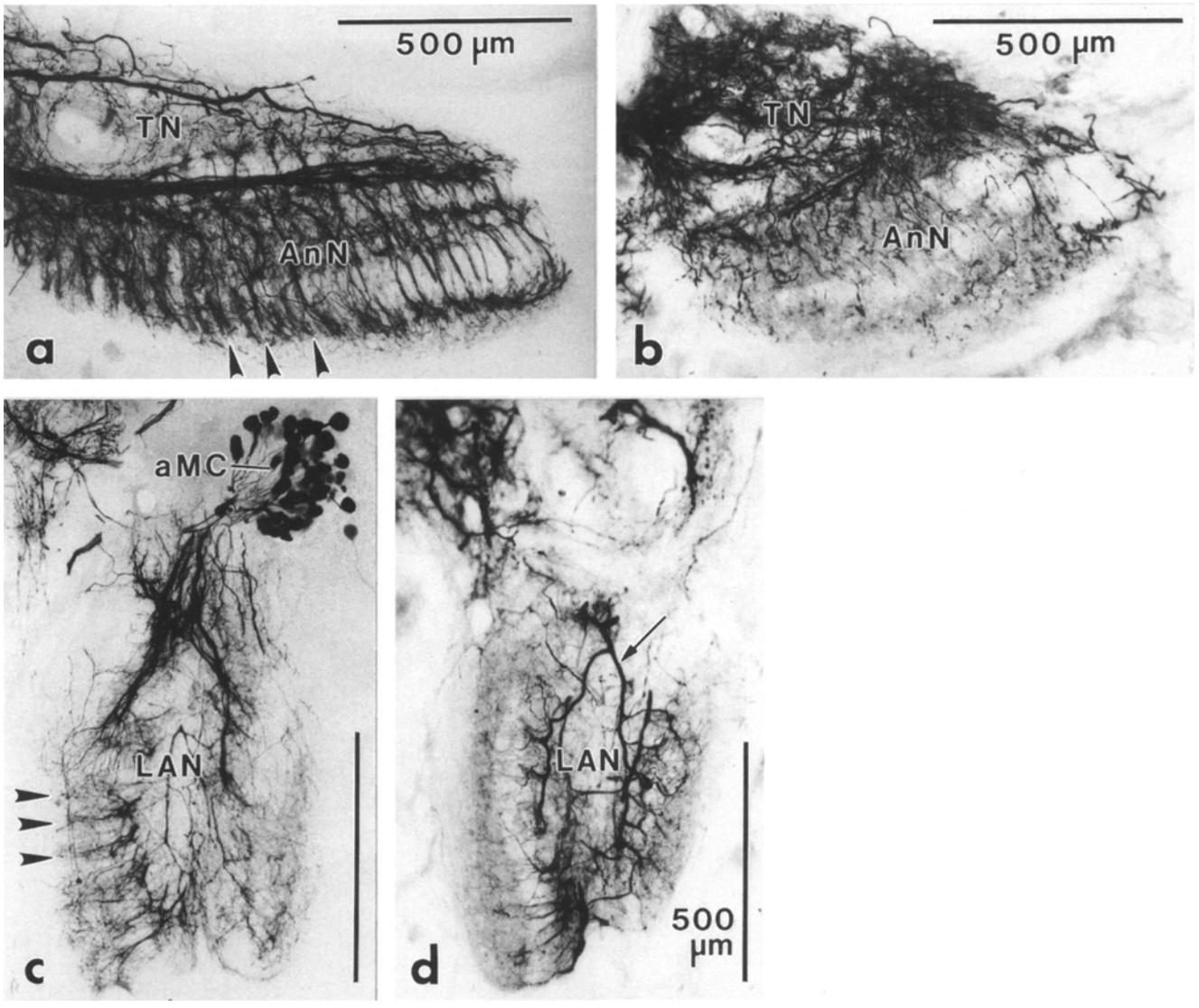

Fig. 17a–d LM micrographs of horizontal vibratome sections showing the innervation pattern of projection neurons in the central brain, visualized by biocytin backfills of the PT (**a, c**) and the OC (**b, d**). **a** Projection neurons with axon in the PT have very dense, regular arborizations in the *AnN* that contribute to the stratification of the neuropil (*arrows*); innervation of *TN* considerably less dense. **b** Projection neurons with axon in the OC have very dense, irregular arborizations in the *TN*; innervation of *AnN* less dense. **c** Projection neurons with axon in the PT have dense, very fine, regular arborizations in both lobes of the *LAN* that contribute to the stratification of the neuropil (*arrows*). This innervation can be mainly attributed to ascending projection neurons of the central brain, since most arborizations are connected to a dorsally located group of somata in the anterior subcluster of the medial cluster (*aMC*). **d** Projection neurons with axon in the OC have less dense, coarser arborizations in the *LAN*. Innervation of the LAN is dominated by one projection neuron with thick neurites and regular side-branches in both lobes

lateral flagellum and 78% (7 of 9) to mechanical stimulation of the medial flagellum, only 53% (16 of 30) of the OL neurons responded to mechanical stimulation of the lateral flagellum and a mere 17% (3 of 18) to mechanical stimulation of the medial flagellum (see accompanying paper). Further, mechanosensitive responses of most "OL neurons" had latencies >200 ms, in contrast to the "LAN/MAN neurons" that were sufficiently fast (<50 ms) to be driven by direct monosynaptic connections to the afferents.

Third, is the extent of sensory-motor integration. Antennular motoneurons (present study; Schmidt and Ache 1993) arborize heavily in the LAN and/or the MAN, but not in the OL or AL, so that only the former could serve as a center for antennular sensory-motor integration. Maynard (1965) earlier showed that antennular motoneurons in the LAN are activated by electrical stimulation of the antennular nerve, but was unable to identify the sensory modalities that provide physiologically relevant input. Our evidence that antennular motoneurons show diverse, often complex responses to chemical stimulation but relatively simple responses to mechanical stimulation suggests that the

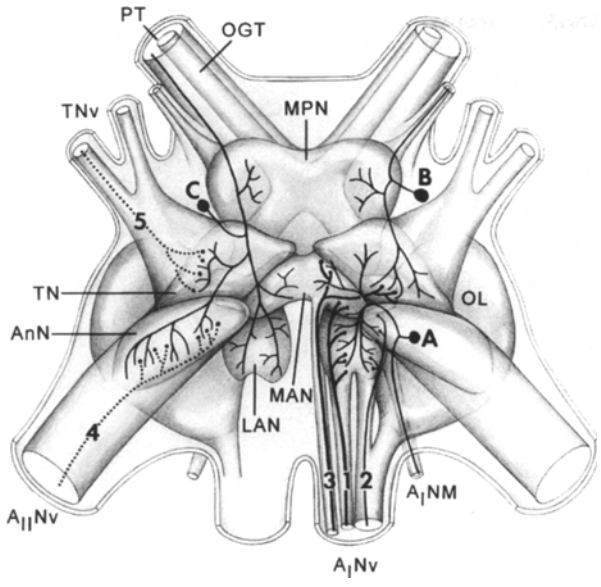

Fig. 18 Summary diagram of the LAN/MAN pathway in the central brain of the spiny lobster. Neurons are drawn idealized to depict regions of overlapping arborizations and thus presumptive sites of synaptic interactions. Sensory afferents are *numbered*, central neurons *labeled with letters*. Central brain is viewed from dorsal; the ventrally located olfactory lobe (*OL*) and the tract of its projection neurons – the olfactory globular tract (*OGT*) – is outlined for reference. *Right side*: Sensory-motor coupling in the lateral (*LAN*) and median antennular neuropils (*MAN*). Mechanosensory (*1*) and presumptive non-olfactory chemosensory afferents (*2*) originating from the medial and lateral antennular flagella primarily arborize in the respective lobes of the LAN. In the LAN, their terminals extensively overlap with and likely synapse on the terminals of antennular motoneurons (*A*; depicted is a type I motoneuron), which have additional arbors in the MAN and the tegumentary neuropil (*TN*) and axons leaving the central brain via the main antennular nerve (A_INv) or the antennular motor nerve (A_INM). Primarily mechanosensory afferents from the statocyst and other mechanoreceptors on the base of the antennule (*3*) target the MAN. In the MAN their terminals overlap with and likely synapse on the terminals of antennular (*A*) and eyestalk motoneurons (*B*). The eyestalk motoneurons have addition arbors in the TN and the median protocerebral neuropils (*MPN*) and axons leaving the central brain via the oculomotor nerve (*OCM*). *Left side*: Projection neurons of the central brain arborizing in the LAN and/or MAN. Ascending (*A*) and descending projection neurons (not depicted) have a similar arborization pattern and mainly differ in the route by which their axons leave the central brain: via the protocerebral tract (*PT*) or via the oesophageal connectives, respectively. Besides their arbors in the LAN and/or MAN that overlap with the terminals of antennular sensory afferents these projection neurons have arbors in the antennal neuropil (*AnN*) overlapping with the terminals of putative antennal sensory afferents (*4*), in the TN overlapping with the terminals of putative tegumentary sensory afferents (*5*), and in the MPN overlapping with the arbors of higher order visual interneurons. Most likely direct mechanosensory and non-olfactory chemosensory input from all sensilla on the head and its appendages together with indirect visual input is integrated in these projection neurons

antennular motoneurons are driven primarily by chemosensory input. Thus, our results extend Maynard's (1965) idea that the LAN is a lower motor center of the antennule to include the MAN and suggest that integration of non-olfactory chemosensory and mechanosensory input from the antennule and motor output driving antennular movements is the sole domain of the LAN/MAN pathway.

Fourth, is the morphological separation of their output neurons. The projection neurons with antennular input in the present study do not arborize in the OL, in contrast with those in the accompanying paper, a distinction seen in previous studies. Projection neurons that exclusively arborize in the OL (and/or the AL) do not branch in any other neuropils of the central brain and have an extremely *thin* axon ascending from the central brain via the olfactory globular tract (Mellon et al. 1992; Mellon and Alones 1993; Sandeman and Sandeman 1994; Wachowiak and Ache 1994; accompanying paper, Schmidt and Ache 1996). On the other hand, projection neurons of the central brain that receive antennular input but lack branches in the OL (and other neuropils of the olfactory deutocerebrum) have a *thick* axon in the protocerebral tract or the oesophageal connectives and as a group arborize in the LAN and/or MAN, the tritocerebrum, and the median protocerebrum (Fig. 18) (Fraser 1974; Fraser and Sandeman 1975; Glantz et al. 1981; Hamilton and Ache 1983; Tautz et al. 1986; Tautz 1987; Arbas et al. 1988; Derby and Blaustein 1988; Nakagawa and Hisada 1989, 1990). Most of these projection neurons have at least minor branches in the LAN and/or MAN, indicating that they receive antennular sensory input via the non-olfactory chemosensory and mechanosensory afferents projecting to these neuropils. Glantz et al. (1981) showed that 83% (35 of 42) of the descending projection neurons of the central brain of crayfish that receive sensory input from the antennule have at least some arborizations in the LAN, whereas none of all 52 descending neurons had any branches in the OL (or related neuropils of the olfactory deutocerebrum). Thus, neurons appear to project independently from each pathway.

There is a morphological substrate for crosstalk between the two pathways through local interneurons, but any such crosstalk would appear to be restricted and indirect. Some local interneurons with a main arbor in the OL (and/or the AL) have minor arborizations in the LAN (Arbas et al. 1988; accompanying paper). Although the direction of information flow in these local interneurons is unknown, it appears unlikely that chemosensory input to the LAN is exclusively provided via this route, as proposed by Derby and Blaustein (1988) since the LAN is directly innervated by numerous presumptive non-olfactory chemosensory afferents. Alternatively, such "crosstalking" local OL interneurons could receive additional non-olfactory input in the LAN and feed it into ongoing integration of olfactory input in the OL. All other local interneurons in the central brain known to receive antennular input arborize in the LAN (Arbas et al. 1988: cell

#13) or the MAN (Nakagawa and Hisada 1991, 1992) and several other neuropils of the trito- and median protocerebrum, but have no branches in the OL (or other neuropils of the olfactory deutocerebrum).

Implications of functional division of the deutocerebrum

To understand the functional organization of the decapod deutocerebrum one must discern which of the two pathways is activating central neurons that respond to chemical stimulation of the antennule. Previous recordings, including those from our lab, specified projection neurons that responded to antennular chemostimulation but had no arborizations in OL as "olfactory interneurons" (Hamilton and Ache 1983; Tautz et al. 1986; Tautz 1987; Arbas et al. 1988; Derby and Blaustein 1988). According to our present results it is much more likely that such neurons are activated via the LAN/MAN pathway and therefore reflect "non-olfactory" chemoreception. The same reinterpretation should be applied to extracellular studies of ascending projection neurons of the central brain responding to chemical stimulation of the antennule (Ache and Fuzessery 1979; Derby and Ache 1984; Derby et al. 1984, 1985). Ascending projection neurons of the olfactory deutocerebrum have extremely thin axons (< 0.3 μm: Mellon et al. 1992; Mellon and Alones 1993; Sandeman and Sandeman 1994; Wachowiak and Ache 1994; accompanying paper) and thus would be underrepresented, if at all present, in extracellular recordings compared to the ascending "LAN/MAN projection neurons", which we show have axons 8–20 μm in diameter. In one of the extracellular studies almost all neurons received chemosensory input from the medial, as well as the lateral, flagellum of the antennule (Derby et al. 1985), and we now show (together with the accompanying paper) that only neurons in the LAN/MAN pathway receive chemosensory input from the medial flagellum.

It is not necessarily obvious how to interpret the responses of higher-order neurons that do not arborize directly in the neuropils in question, such as descending neurons of the eyestalk ganglia (Tautz et al. 1986: cell B; Derby and Blaustein 1988; cells 10 and 11; this study: neurons #7 and 19), neurons with axons in the PT and the OC, which could be descending neurons of the eyestalk ganglia or ascending neurons of the ventral cord (Derby and Blaustein 1988: cells 12 and 13), and ascending projection neurons of the central brain lacking any arborizations in the LAN and MAN (Derby and Blaustein 1988; cells 3 and 7). In these instances, other criteria must be brought to bear. For example, chemoresponsive ascending projection neurons of the central brain that lack branches in the LAN/MAN (Derby and Blaustein 1988: cells 3 and 7) most likely get chemosensory input through the LAN/MAN pathway since they arborize extensively in the median protocerebrum and thereby overlap the arbors of ascending projection neurons of the LAN/MAN pathway.

Functional division of the deutocerebrum in two separate sensory pathways also occurs in insects, the other well-studied group of arthropods (reviews: Rospars 1988; Masson and Mustaparta 1990). The insect antennal lobe is organized in glomeruli and receives and integrates olfactory input from the antenna and therefore can be regarded as equivalent to the crustacean OL. A second, unstructured neuropil, the posterior (or dorsal) lobe appears to receive most or all mechanosensory antennal afferents. Since it also contains the arborizations of antennal motoneurons, the posterior lobe is thought to represent the antennal mechanosensory-motor center (Rospars 1988). As yet, however, there is no evidence that chemosensory input is processed in the posterior lobe of insects, possibly limiting analogy with the crustacean LAN/MAN. Non-olfactory chemosensory, that is gustatory input from the antenna of insects is thought to be pooled with olfactory input in the antennal lobe (Masson and Mustaparta 1990), although the fate of antennal gustatory afferents is not known. Hopefully, our findings will stimulate the search for possible gustatory input to the posterior lobe in insects.

It is tempting to speculate that division of the deutocerebrum into two, functionally distinct sensory pathways reflects, at least in part, differences in how chemosensory information is processed that is fundamental to understanding the origin of the sense of smell as a distinct sensory modality.

Acknowledgements Supported by DFG awards Schm 738/1-1 and Schm 738/1-2 and NSF awards 88-10261 and 92-22765. We thank the late Dr. W. Heiligenberg for originally introducing us to the biocytin method. Without his encouragement this work would not have been possible. We also thank Ms. Leslie van Ekeris for her outstanding technical assistance and Mr. Wilfried Roloff for his expert help with many of the drawings.

References

Ache BW, Fuzessery ZM (1979) Chemosensory integration in the spiny lobster: Ascending activity in the olfactory-globular tract. J Comp Physiol 130: 63–69

Arbas EA, Humphreys CJ, Ache BW (1988) Morphology and physiological properties of interneurons in the olfactory midbrain of the crayfish. J Comp Physiol A 164: 231–241

Blaustein DN, Derby CD, Simmons RB, Beall AC (1988) Structure of the brain and medulla terminalis of the spiny lobster *Panulirus argus* and the crayfish *Procambarus clarkii*, with an emphasis on olfactory centers. J Crust Biol 8: 493–519

Derby CD, Ache BW (1984) Quality coding of a complex odorant in an invertebrate. J Neurophysiol 51(5): 906–924

Derby CD, Blaustein DN (1988) Morphological and physiological characterization of individual olfactory interneurons connecting the brain and eyestalk ganglia of the crayfish. J Comp Physiol A 163: 777–794

Derby CD, Hamilton KA, Ache BW (1984) Processing of olfactory information at three neuronal levels in the spiny lobster. Brain Res 300: 311–319

Derby CD, Ache BW, Kennel EW (1985) Mixture suppression in olfaction: electrophysiological evaluation of the contribution of peripheral and central neural components. Chem Senses 10: 301–316

Fraser PJ (1974) Interneurones in crab connectives (*Carcinus maenas* (L.)): directional statocyst fibres. J Exp Biol 61: 615–628

Fraser PJ, Sandeman DC (1975) Effects of angular and linear accelerations on semicircular canal interneurons of the crab *Scylla serrata*. J Comp Physiol 96: 205–221

Fuzessery ZM (1978) Quantitative stimulation of antennular chemoreceptors of the spiny lobster, *Panulirus argus*. Comp Biochem Physiol 60: 303–308

Glantz RM, Kirk M, Viancour T (1981) Interneurons in the crayfish brain: The relationship between dendrite location and afferent input. J Neurobiol 12: 311–328

Gleeson RA (1982) Morphological and behavioral identification of the sensory structures mediating pheromone reception in the blue crab, *Callinectes sapidus*. Biol Bull 163: 162–171

Grünert U, Ache BW (1988) Ultrastructure of the aesthetasc (olfactory) sensilla of the spiny lobster, *Panulirus argus*. Cell Tissue Res 251: 95–103

Hamilton KA, Ache BW (1983) Olfactory excitation of interneurons in the brain of the spiny lobster. J Comp Physiol 150: 129–140

Helm F (1928) Vergleichend-anatomische Untersuchungen über das Gehirn, insbesondere das "Antennalganglion" der Dekapoden. Z Morph Ökol Tiere 12: 70–134

Horikawa K, Armstrong WE (1988) A versatile means of intracellular labeling: injection of biocytin and its detection with avidin conjugates. J Neurosci Methods 25: 1–11

Kouyama N, Shimozawa T (1982) The structure of a hair mechanoreceptor in the antennule of crayfish (Crustacea). Cell Tissue Res 226: 565–578

Laverack MS (1964) The antennular sense organs of *Panulirus argus*. Comp Biochem Physiol 13: 301–321

Masson C, Mustaparta H (1990) Chemical information processing in the olfactory system of insects. Physiol Rev 70: 199–245

Maynard DM (1965) Integration in crustacean ganglia. Symp Soc Exp Biol 20: 111–149

Maynard DM, Dingle H (1963) An effect of eyestalk ablation on the antennular function in the spiny lobster, *Panulirus argus*. Z Vergl Physiol 46: 515–540

Mellon D Jr (1977) Central and peripheral features of crayfish oculomotor organization. In: Hoyle G (ed) Identified neurons and behavior of arthropods. Plenum Press, New York London, pp 149–166

Mellon D Jr, Alones V (1993) Cellular organization and growth-related plasticity of the crayfish olfactory midbrain. Microsc Res Tech 24: 231–259

Mellon D Jr, Munger SD (1990) Nontopographic projection of olfactory sensory neurons in the crayfish brain. J Comp Neurol 296: 253–262

Mellon D Jr, Alones V, Lawrence MD (1992) Anatomy and fine structure of neurons in the deutocerebral projection pathway of the crayfish olfactory system. J Comp Neurol 321: 93–111

Michel WC, Trapido-Rosenthal HG, Chao ET, Wachowiak M (1993) Stereoselective detection of amino acids by lobster olfactory receptor neurons. J Comp Physiol A 171: 705–712

Nakagawa H, Hisada M (1989) Morphology of descending statocyst interneurons in the crayfish *Procambarus clarkii* Girard. Cell Tissue Res 255: 539–551

Nakagawa H, Hisada M (1990) A vibration-sensitive descending statocyst interneurone in the crayfish *Procambarus clarkii*. J Exp Biol 149: 361–378

Nakagawa H, Hisada M (1991) Inhibitory connections underlying the directional sensitivity of the equilibrium system in the crayfish *Procambarus clarkii*. J Exp Biol 152: 305–312

Nakagawa H, Hisada M (1992) Local spiking interneurons controlling the equilibrium response in the crayfish *Procambarus clarkii*. J Comp Physiol A 170: 291–302

Neil DM (1982) Compensatory eye movements. In: Sandeman DC, Atwood HL (eds) The biology of Crustacea, vol. 4. Neural integration and behavior. Acad Press, New York London, pp 133–163

Patton ML, Grove RF (1992) The response of statocyst receptors of the lobster, *Homarus americanus*, to movements of statolith hairs. Comp Biochem Physiol 101A: 249–257

Rospars JP (1988) Structure and development of the insect antennodeutocerebral system. Int J Insect Morphol Embryol 17: 243–294

Roye DB (1975) The physiological basis for pitch-induced antennule movements in the blue crab, *Callinectes sapidus*. Comp Biochem Physiol 62A: 475–484

Roye DB (1986) The central distribution of movement sensitive afferent fibers from the antennular short hair sensilla of *Callinectes sapidus*. Mar Behav Physiol 12: 181–196

Roye DB, Dillaman RM (1982) Morphological and physiological characteristics of the antennular short hair sensilla of the blue crab, *Callinectes sapidus*. Mar Behav Physiol 9: 59–71

Sandeman DC, Denburg JL (1976) The central projections of chemoreceptor axons in the crayfish revealed by axoplasmic transport. Brain Res 115: 492–496

Sandeman DC, Luff SE (1973) The structural organization of glomerular neuropile in the olfactory and accessory lobes of an Australian freshwater crayfish, *Cherax destructor*. Z Zellforsch 142: 37–61

Sandeman DC, Okajima A (1972) Statocyst-induced eye movements in the crab *Scylla serrata*. I. The sensory input from the statocyst. J Exp Biol 57: 187–204

Sandeman DC, Okajima A (1973) Statocyst-induced eye movements in the crab *Scylla serrata*. III. The anatomical projections of sensory and motor neurones and the responses of the motor neurones. J Exp Biol 59: 17–38

Sandeman DC, Sandeman RE (1994) Electrical responses and synaptic connections of giant serotonin-immunoreactive neurons in crayfish olfactory and accessory lobes. J Comp Neurol 341: 130–144

Sandeman D, Sandeman R, Derby C, Schmidt M (1992) Morphology of the brain of crayfish, crabs, and spiny lobsters: A common nomenclature for homologous structures. Biol Bull 183: 304–326

Schmidt M, Ache BW (1992) Antennular projections to the midbrain of the spiny lopbster. II. Sensory innervation of the olfactory lobe. J Comp Neurol 318: 291–303

Schmidt M, Ache BW (1993) Antennular projections to the midbrain of the spiny lopbster. III. Central arborizations of motoneurons. J Comp Neurol 336: 583–594

Schmidt M, Ache BW (1996) Processing of antennular input in the brain of the spiny lobster, *Panulirus argus*. II. The olfactory pathway. J Comp Physiol A

Schmidt M, Orona E, Ache BW (1991) Parallel processing of chemosensory input in the brain of the spiny lobster. Soc Neurosci Abstr 17: 1018

Schmidt M, Van Ekeris L, Ache BW (1992) Antennular projections to the midbrain of the spiny lobster. I. Sensory innervation of the lateral and medial antennular neuropils. J Comp Neurol 318: 277–290

Silvey GE, Sandeman DC (1976) Integration between statocyst sensory neurons and oculomotor neurons in the crab *Scylla serrata*. III. The sensory to motor synapse. J Comp Physiol 108: 53–65

Silvey GE, Dunn PA, Sandeman DC (1976) Integration between statocyst sensory neurons and oculomotor neurons in the crab *Scylla serrata*. II. The thread hair sensory receptors. J Comp Physiol 108: 45–52

Snow PJ (1973) The antennular activities of the hermit crab, *Pagurus alaskensis* (Benedikt). J Exp Biol 58: 745–765

Snow PJ (1974) Surface structures of the antennular flagella of the hermit crab *Pagurus alaskensis* (Benedict): A light and scanning electron microscopy study. J Morphol 144: 195–216

Spencer M (1986) The innervation and chemical sensitivity of single aesthetasc hairs. J Comp Physiol A 158: 59–68

Spencer M, Linberg KA (1986) Ultrastructure of aesthetasc innervation and external morphology of the lateral antennule setae of the spiny lobster *Panulirus interruptus* (Randall). Cell Tissue Res 245: 69–80

Tautz J (1987) Interneurons in the tritocerebrum of the crayfish. Brain Res 407: 230–239

Tautz J, Erber J, Ache B (1986) Chemosensitive interneurons ascend in the optic nerve in the crayfish. Naturwissenschaften 73: 154–155

Tierney AJ, Voigt R, Atema J (1988) Response properties of chemoreceptors from the medial antennular filament of the lobster *Homarus americanus*. Biol Bull 174: 364–372

Wachowiak M, Ache BW (1994) Morphology and physiology of olfactory projection neurons in the spiny lobster: J Comp Physiol A 175: 35–48

Wyse GA, Maynard DM (1965) Joint receptors in the antennule of *Panulirus argus* Latreille. J Exp Biol 42: 521–535

Yoshino M, Kondoh Y, Hisada M (1983) Projection of statocyst sensory neurons associated with crescent hairs in the crayfish *Procambarus clarkii* Girard. Cell Tissue Res 230: 37–48